

Multi-messenger astrophysics

Péter Mészáros^{1,2,3,4*}, Derek B. Fox^{1,3,4}, Chad Hanna^{1,2,3,4} and Kohta Murase^{1,2,3,4,5}

Abstract | Multi-messenger astrophysics, a long-anticipated extension to traditional multiwavelength astronomy, has emerged over the past decade as a distinct discipline providing unique and valuable insights into the properties and processes of the physical Universe. These insights arise from the inherently complementary information carried by photons, gravitational waves, neutrinos and cosmic rays about individual cosmic sources and source populations. This complementarity is the reason why multi-messenger astrophysics is much more than just the sum of the parts. In this Review article, we survey the current status of multi-messenger astrophysics, highlighting some exciting results, and discussing the major follow-up questions they have raised. Key recent achievements include the measurement of the spectrum of ultrahigh-energy cosmic rays out to the highest observable energies; the discovery of the diffuse high-energy neutrino background; the first direct detections of gravitational waves and the use of gravitational waves to characterize merging black holes and neutron stars in strong-field gravity; and the identification of the first joint electromagnetic plus gravitational wave and electromagnetic plus high-energy neutrino multi-messenger sources. We discuss the rationales for the next generation of multi-messenger observatories, and outline a vision of the most likely future directions for this exciting and rapidly growing field.

Until the mid-twentieth century, of the four fundamental forces in nature — the electromagnetic (EM), gravitational, weak and strong nuclear forces — it was only messengers of the EM force, in the form of optical photons, that astronomers could use to study the distant Universe. Technological advances provided access to radio, infrared, ultraviolet, X-ray and γ -ray photons. But only in the past few decades, the messengers of the other three forces, namely gravitational waves (GWs), neutrinos and cosmic rays, could be used in astronomical observations. Thus, we are now finally using the complete set (as far as known) of the forces of nature, which are revealing exciting and hitherto unknown facts about the cosmos and its denizens.

Compared with most EM emissions, these new non-photonic messengers are generally more challenging to detect and to trace back to their cosmic sources. When detected, they are usually associated with extremely high-mass or high-energy-density configurations (for example, the dense core of normal stars, stellar explosions at the end of the life of massive stars, the surface neighbourhood of extremely compact stellar remnants such as white dwarfs, neutron stars or black holes, the strong and fast-varying gravitational field near either stellar mass black holes or the more massive black holes in the core of galaxies, or in energetic shocks in high-velocity plasmas associated with compact astrophysical sources). This association with the most violent

astrophysical phenomena known means that the interpretation of observations enabled by multiple messengers requires, and can have implications for, our theories of fundamental physics, including strong-field gravity, nuclear physics and particle interactions.

The study of such high-energy compact objects started in the 1950s, after decades of a slow build-up with increasingly larger ground-based optical telescopes. The first major breakthrough came from the deployment of large radio-telescopes, followed by the launch of satellites equipped with X-ray and later γ -ray detectors, which established the existence of active galactic nuclei (AGN), neutron stars and black holes, and revealed dramatic high-energy transient phenomena, including X-ray novae, X-ray bursts and gamma-ray bursts (GRBs).

In the late 1960s, large underground neutrino detectors were built, first measuring the neutrinos produced in the Sun and later those arising from a supernova explosion (see joint multi-messenger results section below). It was only in the current decade that extragalactic neutrinos in the TeV to PeV range were discovered^{1,2}. Cosmic rays in the GeV energy range started to be measured in the 1910s, but it was only in the 1960s that large detectors started measuring higher energies, suggesting an extragalactic origin, and only in the past decade has it become practical to start investigating the spectrum and composition in the 10^{18} – 10^{20} eV energy range, for example, see REF.³. GW detectors were first built in the 1970s, but it was not

¹Department of Astronomy and Astrophysics, Pennsylvania State University, University Park, PA, USA.

²Department of Physics, Pennsylvania State University, University Park, PA, USA.

³Center for Particle and Gravitational Astrophysics, Pennsylvania State University, University Park, PA, USA.

⁴Institute for Gravitation and the Cosmos, Pennsylvania State University, University Park, PA, USA.

⁵Center for Gravitational Physics, Yukawa Institute for Theoretical Physics, Kyoto University, Kyoto, Japan.

*e-mail: nnp@psu.edu

<https://doi.org/10.1038/s42254-019-0101-z>

Key points

- Besides the traditional electromagnetic observations, multi-messenger astrophysics uses the information about the astrophysical Universe provided by the gravitational, weak and strong forces. These new channels provide untapped, qualitatively different and **complementary types of information**, making previously hidden objects visible.
- Diffuse backgrounds** of high-energy neutrinos (HENs) with energies from ~ 10 TeV to PeV, ultrahigh-energy cosmic rays (UHECRs) at energies up to $\sim 10^{20}$ eV and γ -rays with energies between MeV and \sim TeV have been measured, or upper limits have been provided, by Cherenkov detectors, satellites and ground-based air shower arrays.
- Gravitational waves** from merging stellar mass black hole and neutron star binaries have been detected at frequencies in the ~ 10 Hz to ~ 1 kHz range with **laser interferometric gravitational wave detectors**.
- The sources of the diffuse UHECR and HEN backgrounds remain unknown**, although a γ -ray-flaring blazar has been tentatively identified with the observed HENs. Although up to $\sim 85\%$ of the γ -ray background can be attributed to blazars, it appears that at most 30% of the HEN background has the same origin.
- The natural physical **connection between high-energy cosmic ray interactions and the resulting very-high-energy neutrinos and γ -rays can provide clues about their unknown astrophysical sources**. Although less direct, the connection with gravitational wave emission is expected to provide important information about supermassive black hole populations and dynamics.
- The advanced gravitational wave detectors will soon be able to detect hundreds of binary mergers up to \sim Gpc distances, but electromagnetic counterpart searches rely primarily on the aging space-based facilities Swift and Fermi, currently operating well beyond their design lifetimes. **There is an urgent need for a new generation of electromagnetic detectors**, extending the range of frequencies.

Neutron stars

The remnant of a core-collapse supernova from a star in the ~ 8 – $25 M_{\odot}$ mass range, whose central core of mass ~ 0.5 – $2.0 M_{\odot}$ collapsed to a radius of ~ 10 km consisting mainly of neutrons.

Stellar mass black holes

Thought to arise in core-collapse supernova from stars $\gtrsim 25 M_{\odot}$, whose collapsed core has a mass greater than the maximum allowed for stable neutron star, resulting instead in a black hole of a neutron star.

Active galactic nuclei

A type of galaxies whose nuclear region, harbouring an accreting massive black hole, is so bright that it outshines the rest of the galaxy.

Gamma-ray bursts

A sudden, brief, extremely luminous sources of mainly γ -rays.

Supernova

An intense stellar explosion, leading to a rapid brightening of the optical emission by more than ten orders of magnitude, followed by a gradual dimming. There are two basic subtypes, core-collapse supernovae and type Ia (nuclear deflagration) supernovae.

until the 1990s that the sensitivity required for detection was achieved owing to new technologies and sufficiently large arrays. **The first GW detections⁴ came in 2015.**

Mono-messengers and multi-messengers

In this section, we overview experimental results that confirm many of the theoretical and phenomenological predictions and expectations formulated over the past several decades. **Schematic representations of some of the sources detected so far, and some that are suspected but not detected so far, are presented in BOX 1.**

Mono-messenger results

Here we highlight some of the major recent results relying only on a single type of messengers, such as cosmic rays (strong force), neutrinos (weak force), GWs (gravitational force) or photons (electromagnetic force).

Ultrahigh-energy cosmic rays. The Pierre Auger cosmic ray observatory⁵ in Argentina is a 3,000 km² array of 1,660 water Cherenkov stations and 27 air fluorescence telescopes (FIG. 1), designed to detect ultrahigh-energy cosmic rays (UHECRs) at energies between 10^{17} eV and 10^{21} eV. **Its measurements of the diffuse UHECR flux energy spectrum, which began in 2009, confirmed the existence of a spectral steepening (a drop-off in the number of UHECRs) occurring³ above $\sim 6 \times 10^{19}$ eV, which had been first observed by the HiRes instrument⁶. This is consistent with the so-called Greisen–Zatsepin–Kuzmin (GZK) feature^{7,8} expected from cosmic ray proton energy losses or from heavy-ion photodissociation⁹ due to interactions with cosmic microwave background photons. An alternative explanation for the origin of the spectral steepening could be due to cosmic rays protons reaching a maximum acceleration at the sources.**

From 2010, the Pierre Auger Observatory began showing evidence for the chemical composition of UHECRs becoming heavier (an increased presence of larger atomic numbers $A > 1$) above $\sim 10^{18.5}$ eV. The statistical significance of these results has increased over the years^{10–12}. The spectral results are consistent, within statistical uncertainties, with those obtained with the smaller Telescope Array UHECR Observatory¹³, which is important because the Pierre Auger Observatory is in the Southern Hemisphere whereas the Telescope Array is in the Northern Hemisphere. **The chemical composition of UHECRs is still debated¹⁴, although a joint Pierre Auger–Telescope Array paper¹⁵ reported results that agree within the errors.**

The angular resolution in the arrival direction of UHECRs is below 1° above $\sim 10^{19}$ eV for both protons and heavy elements, although the magnetic deflection increases with mass. Around 10^{19} eV it is $\sim 5^\circ$ for protons, whereas for heavy nuclei it could be tens of degrees. At these energies, due to the energy losses caused by the GZK effect mentioned above, the UHECRs must have originated within distances of ~ 100 Mpc. So far, all attempts to find angular spatial correlations between UHECRs and any type of known cosmic sources have been unsuccessful³. JAIME

High-energy neutrinos. The IceCube neutrino observatory¹⁶ consists of a cubic kilometre (roughly a gigaton) of ice at a depth between 1.4 km and 2.4 km below the South Pole, instrumented with 86 strings connecting 5,160 optical phototubes (FIG. 1), which measure the light radiated from charged particles produced by passing high-energy neutrinos (HENs) interacting with the ice. Its construction was finished in 2010, and in 2012–2013 it discovered a diffuse flux of neutrinos in the range $100 \text{ TeV} \sim E_{\nu} \sim 1 \text{ PeV}$ (REFS^{1,2}), where E_{ν} is the neutrino energy, later extended to 100 TeV. **The energy spectrum dN/dE_{ν} , where N is the number of detected neutrinos, can be fitted to an ~ -2.5 index power law, but there may be an indication for the existence of two components, one steeper, below ~ 500 TeV (index ~ -2.5), and one flatter (index ~ -2) above that, the highest energy so far being ~ 10 PeV. IceCube can detect all neutrino flavours, with muon neutrino charged current interactions resulting in elongated Cherenkov tracks and all other neutrino flavours and interactions largely producing near-spherical optical Cherenkov signals from secondary particle cascades, the direction of arrival being uncertain by ~ 10 – 15° for cascades and ~ 0.5 – 1.0° for tracks. At sufficiently high energies, at which the statistics are lower, tau neutrinos have not yet been identified, but a suggested tau-like candidate has been discussed¹⁷. The observed flavour distribution is compatible with complete flavour mixing having occurred due to the neutrino oscillation phenomenon (BOX 2) over cosmological distances^{18,19}. So far, there is no obvious correlation between the observed neutrinos and any type of known cosmic objects²⁰, except for one interesting case discussed in the following subsection.**

The smaller underwater Cherenkov telescopes ANTARES²¹ and the Baikal Detector (Baikal-GVD)²² have also been in operation and providing complementary

Box 1 | Multi-messengers and their interrelations

A multi-messenger source might emit two, three or even all four different types of messengers. From a binary neutron star merger (panel **a** of the figure), such as the GW/GRB 170817 event, two types of multi-messengers, gravitational waves (GW) and photons (γ), were observed^{54,57,59}, the latter indicating that the source was a short gamma-ray burst (GRB). Such sources may also emit high-energy neutrinos (HENs) and cosmic rays (CRs)^{84,85,168}, although for the GW/GRB 170817 event, theories predict such fluxes to be too low for current detectors. If this is true, it will take closer binary neutron star merger events or next-generation HEN facilities to observe HENs from these sources. The so-called long GRBs (panel **b** of the figure) also may emit HENs and CRs, which so far have not been detected, while their GW emission is expected to be very low.

Another example is a tidal disruption event (TDE) of a star by a massive black hole (panel **c** of the figure). In this case, shocks in the disrupted gas can accelerate particles and lead to CRs and HENs^{169–172}. TDEs involving white dwarf stars and $\sim 10^4 M_{\odot}$ (where M_{\odot} is solar mass) black holes lead to strong low-frequency (~ 1 mHz) GW emission that could be observed by the forthcoming evolved Laser Interferometer Space Antenna (eLISA) mission. A solitary supermassive black hole with a jet may emit γ -rays, HEN and CRs (panel **d** of the figure), as it is suspected in the case of the 2017 flaring episode of the BL Lac-type blazar TXS 0506+056 (REFS^{65–68,71,72}).

In general, in compact mergers, TDEs and related sources, the co-production of CRs, HEN and high-energy γ -rays is anticipated, as the physics of these three messengers are closely connected: shocks and the high-energy particle acceleration lead to the interaction of highly relativistic protons (or nuclei) with ambient gas or intense radiation fields, resulting in neutrinos, γ -rays and electrons/positrons.

For single objects, even those of extreme mass and undergoing substantial accretion, relatively weak GW emission is expected as the time-varying quadrupole moment (which requires the breaking of azimuthal symmetry) is thought to be small in these cases. The sole exception would be an engine-driven supernova, or a plain supernova, located in our galaxy (panels **e** and **f** of the figure), which would be sufficiently close such that the detection of coherent or incoherent GWs by current and future ground-based detectors is anticipated. IceCube is well equipped for detecting thermal (~ 10 MeV) neutrinos from such galactic supernovae. A challenge for theory is to predict the amplitude and spectrum of the GW and neutrinos from different types of supernovae.

Strong GW emissions have been observed from the mergers of compact binary systems, either from two merging stellar mass black holes (panel **g** of the figure)²⁷, two merging neutron stars (panel **a**)⁵⁴ or black hole–neutron star mergers, because the final inspiral to coalescence yields a strong GW signal in the ‘sweet spot’ frequency range for ground-based GW detectors. In the case of $30 M_{\odot} + 30 M_{\odot}$ black hole binary systems, such coalescence events can already be observed out to ~ 500 Mpc distances¹⁴¹. However, in the case of black hole–black hole mergers little electromagnetic (EM) flux is expected, because the ambient matter density (protons, electrons) in the vicinity of the binary, at the time of the merger, is typically very low. A key exception are accreting supermassive black holes at the centres of massive galaxies, which are expected to merge in the wake of the coalescence of their component galaxies. These supermassive black holes mergers are key targets for the eLISA mission, and may well exhibit accompanying EM, CR and HEN emission¹⁷³.

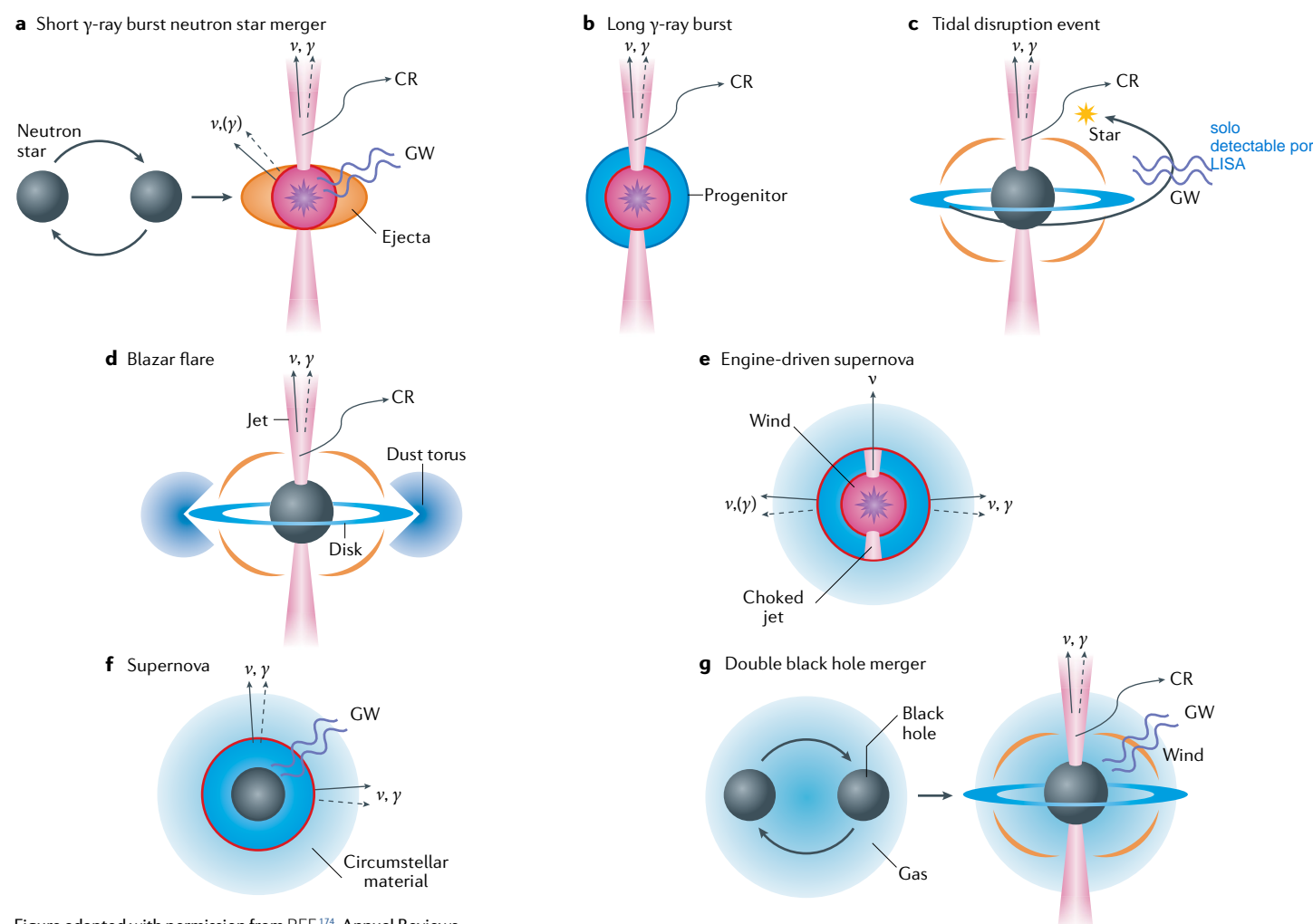


Figure adapted with permission from REF.¹⁷⁴, Annual Reviews.

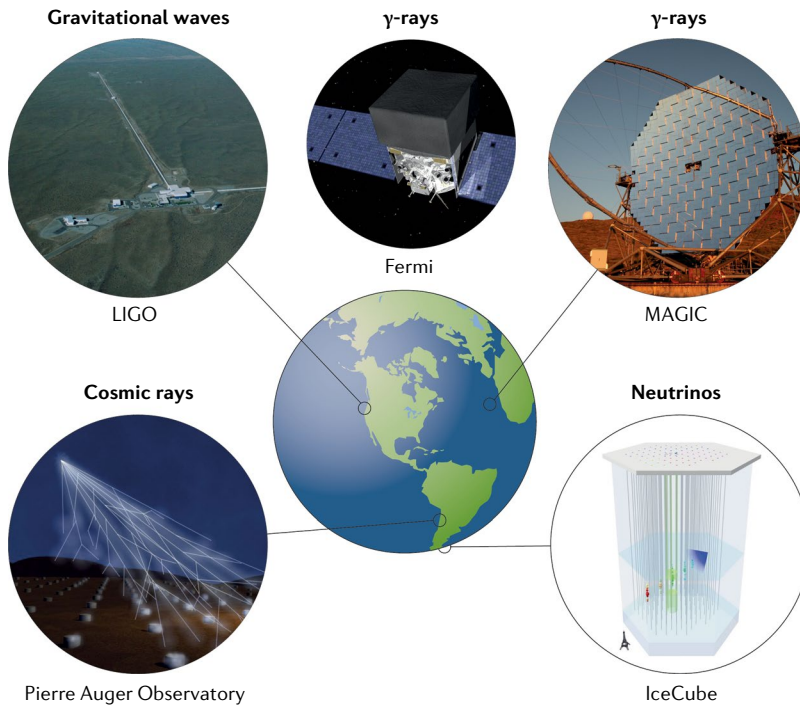


Fig. 1 | Examples of current instruments observing cosmic messengers via the electromagnetic, gravitational, weak and strong forces. The Laser Interferometer Gravitational-Wave Observatory (LIGO) Hanford site in Washington, USA (Courtesy Caltech/MIT/LIGO Laboratory), the Fermi γ -ray space telescope (Credit: NASA), one of the Major Atmospheric Gamma Imaging Cherenkov Telescopes (MAGIC) telescopes situated at the Roque de los Muchachos Observatory on La Palma, Canary Islands (Credit: MAGIC collaboration and Robert Wagner), a schematic of the Pierre Auger cosmic ray observatory in Argentina (Courtesy ASPERA/G.Toma/A.Saftoiu) and a schematic of the IceCube cubic kilometre neutrino detector in Antarctica (Credit: IceCube Collaboration).

Blazars

A type of active galactic nucleus where accretion to the central massive black hole leads to ejection of relativistic plasma jet pointing close to the line of sight to the external observer.

Air Cherenkov imaging telescopes

A steerable telescope measuring secondary optical photons produced by high-energy γ -rays impacting the upper Earth atmosphere.

Core-collapse supernova

The end result of the evolution of a star of mass 8 that has exhausted its nuclear fuel burning capacity, leading to the gravitational collapse of its inner core and the ejection of its outer envelope.

information for the neutrino flux. At much higher energies, the high-altitude balloon experiment Antarctic Impulsive Transient Antenna (ANITA)²³, flying in a circumpolar orbit in Antarctica, used a radio technique to measure neutrinos at $\sim 10^{17}$ eV, which is starting to provide constraints on cosmological neutrino sources and the GZK-related cosmogenic neutrino fluxes, complementary with those provided by the Pierre Auger Observatory²⁴.

Gravitational waves. The Laser Interferometric Gravitational-Wave Observatory (LIGO) consist of two detectors each with 4-km-long L-shaped arms (FIG. 1), which in 2015 began operation in the ~ 10 – 10^3 Hz frequency range²⁵. Another GW observatory, Virgo²⁶ located in Italy, and similarly L-shaped with 3-km-long arms, has been operating at similar times to LIGO, in particular in the second and third operating runs (2016–2017 and 2019 to present). Both instruments will achieve design sensitivity in the coming years (TABLE 1). The long-awaited first discovery of GWs from a stellar mass binary black hole (BBH) merger (labelled GW150914) was announced by LIGO in 2016 (REF. 4; FIG. 2). This was soon followed by a number of other BBH mergers detected both by LIGO and, with lower statistical significance, by Virgo²⁷. The observed black holes weigh up to several tens of solar masses, and have low spins.

So far, despite intensive searches, no other messengers associated with BBH mergers have been detected, except for a possible GRB²⁸ at the time of event GW150914.

Electromagnetic messengers. Except for BBHs, all the other sources detected with the above messengers had been previously extensively studied through their EM emissions at various wavelengths. Important examples of recent observations include those in the optical/ultraviolet, X-ray and up to 150 keV γ -rays with the Swift satellite, and between 10 keV X-rays to \sim TeV γ -rays with the Fermi satellite²⁹ (FIG. 1), which detected a large number of GRB sources, AGN (including blazars), supernovae and a diffuse cosmic γ -background. The ground-based air Cherenkov imaging telescopes, such as the Major Atmospheric Gamma Imaging Cherenkov Telescopes (MAGIC) (FIG. 1), the High Energy Stereoscopic System (HESS), the Very Energetic Radiation Imaging Telescope Array System (VERITAS)³⁰ and the High Altitude Water Cherenkov Observatory (HAWC)^{31,32}, which measure γ -rays in the 100 GeV to multi-TeV range are also very important for the study of these sources. The above have been amply supported by ground and space observations with multiple radio, infrared, optical and ultraviolet telescopes.

Joint multi-messenger results

Solar and supernova neutrinos and photons. The earliest multi-messenger detections involved neutrinos in the MeV range. In the 1960s, a team led by Raymond Davies detected the electron neutrinos produced by the nuclear reactions taking place in the Sun, using a 600 t tank filled with perchlorethylene (cleaning fluid) located deep underground in the Homestake mine in South Dakota, USA. This neutrino flux was confirmed by various other experiments, including the one led by Masatoshi Koshiba in the Kamioka mine in Japan. These discoveries earned Davies and Koshiba the Nobel Prize in Physics in 2002 (REFS^{33,34}).

Another multi-messenger detection was that of neutrinos from a core-collapse supernova (SN 1987a). The neutrinos were produced in an inverse beta decay in which protons are converted into neutrons. The supernova neutrinos were detected by three different underground experiments, Kamiokande in Japan, Baksan in the Soviet Union and Irvine–Michigan–Brookhaven in the United States^{35–37}. This detection preceded by two hours the spectacular optical brightening characterizing the supernova.

Cosmic ray, γ -ray and neutrino background interdependences. The measurements of the diffuse UHECR energy spectrum by the Pierre Auger Observatory established a spectral cut-off above $10^{19.5}$ eV, compatible with what is expected from the GZK energy losses due to the cosmic microwave background photons³. Then, from 2008, the Fermi satellite (following on previous work by the COS-B and other missions) measured a diffuse γ -ray background extending into the sub-TeV range³⁸. In 2012–2013 IceCube discovered, with increasing amount of detail, a diffuse HEN background of astrophysical origin at multi-TeV to PeV energies^{1,2}. Currently, there

Box 2 | Neutrino production and oscillations

The interaction of cosmic ray protons p_{cr} with target protons p_t and target photons γ_t results in a reduced-energy proton p or neutron n , and two intermediate charged or neutral short-lived unstable particles, such as pions $\pi^{\pm,0}$, muons μ^{\pm} , neutrons n and (at higher energies) kaons K^{\pm} , which decay into neutrinos ν_i of different flavours i , γ -rays and electrons or positrons e^{\pm} . Cosmic ray nucleons are primarily subject to spallation against target protons and photodisintegration against target photons, both processes resulting in smaller nucleons including protons and the latter subsequently undergoing the same above mentioned interactions.

$$p_{cr} + p_t/\gamma_t \rightarrow p/n + \pi^+ + \pi^0 + K^+ + \dots$$

$$\begin{aligned}\pi^+ &\rightarrow \mu^+ + \nu_\mu \\ \mu^+ &\rightarrow e^+ + \nu_e + \bar{\nu}_\mu\end{aligned}$$

$$\begin{aligned}\pi^- &\rightarrow \mu^- + \bar{\nu}_\mu \\ \mu^- &\rightarrow e^- + \bar{\nu}_e + \nu_\mu\end{aligned}$$

$$\begin{aligned}\pi^0 &\rightarrow \gamma + \gamma \\ K^+/\bar{K}^- &\rightarrow \mu^+/\mu^- + \nu_\mu/\bar{\nu}_\mu \\ n &\rightarrow p + e^- + \bar{\nu}_e\end{aligned}$$

The primary cosmic ray proton's mean relative energy loss per interaction, called the inelasticity, is $\kappa_{pp} \approx 0.5$ for pp (or pn) and $\kappa_{p\gamma} \approx 0.2$ for $p\gamma$ interactions. For p_{cr} interactions with target protons (or target neutrons), the mean ratio of charged to neutral pion secondaries is $r_{\pm/0} \approx 2$, and for interactions with target photons it is $r_{\pm/0} \approx 1$. The electrons and positrons e^{\pm} quickly lose their energy through synchrotron radiation or inverse Compton scattering, resulting in a further emission of γ -rays, so the final result of the $p_{cr} + p_t/\gamma_t$ interactions are high-energy neutrinos ν_i and γ -rays. The mean energy of the resulting neutrinos and γ -rays is ~ 0.05 and ~ 0.1 of the initial cosmic ray proton's energy. Once neutrinos of any flavour are produced, during their travel from the source to the observer, the neutrinos of any flavour can change into neutrinos of any of the three flavours, in the so-called neutrino oscillation phenomenon. As a result, independently of the ratio of neutrino flavours initially produced at the source where the cosmic ray interactions took place, after travelling over astronomical distances typically all three neutrino flavours are present when they reach the observer. For the neutrino sources considered here, the observable neutrino flavours are expected to be oscillation averages due to the large source distances and the finite energy resolution of the neutrino observatories.

is no firm identification of the sources of either the UHECR, HENs or γ -ray diffuse backgrounds, although the extragalactic γ -ray background is known to be dominated by blazars³⁹. However, theoretical relationships and mutual constraints are expected from the basic physics of these three messengers (FIG. 2).

The HENs are produced when UHECRs collide with low-energy target photons and nuclei resulting in charged and neutral pions, which decay in a predictable fraction of HENs and γ -rays. The resulting energy spectra of neutrinos and photons imply corresponding diffuse backgrounds, which must fit the observed results, also including the constraint provided by the observed UHECR background. The fact that the energetics of these three messengers is comparable can be expressed as a unification of high-energy cosmic particle fluxes (see, for example, REFS^{40,41}). Furthermore, significant constraints are also placed on generic proton–proton hadro-nuclear production models of HENs and γ -rays when they are compared with the Fermi diffuse γ -ray

flux, especially accounting for the $\gamma\gamma$ cascades initiated by γ -rays scattering off cosmic photon radiation backgrounds^{42,43}. The constraints are more stringent for galactic sources⁴⁴. HAWC³¹ is expected to uniquely contribute to measurements of the γ -ray background in the 10–100 TeV energy range, which could strongly constrain the fraction of IceCube neutrinos from galactic origin. Among proton- γ photo-meson production models of HENs, significant constraints have been placed on the contribution of the simpler classical GRB neutrino emission models^{45–47}, while leaving open the possibility of contributions from choked GRBs or supernovae driven by choked jets^{47–49}.

Gravitational waves and photons from binary neutron star mergers. As the culmination of a long series of previous binary neutron star GW/multi-messenger searches (for example, REFS^{50–53}), the joint GW/EM detection of the transient GW/GRB 170817 was the first high significance proof of the strength of the joint multi-messenger technique involving the GW sector⁵⁴ (FIG. 2).

The GWs in GW/GRB 170817 showed that this was a neutron star binary merger, serving to measure the two masses and the distance⁵⁵ and putting constraints on the neutron star equation of state⁵⁶. Meanwhile γ -ray and X-ray measurements by Fermi and Swift showed that it was an off-axis short GRB⁵⁷. The near-simultaneous observation of EM and GW signals from GW/GRB 170817 showed that they both travel at the speed of light to better than 1 part in 10^{15} , thereby ruling out many alternative theories of gravity. Optical observations with various telescopes showed that the merger also manifested itself as a kilonova, which is an outflow rich in the so-called *r*-process high-atomic-number nuclear elements, providing a source for the elements heavier than iron in the Universe (for example, REFS^{58–61}). For their role in the discovery of binary gravitational wave sources Barry C. Barish, Kip S. Thorne and Rainer Weiss received the 2017 Nobel Prize in Physics^{62–64}.

High-energy neutrinos and γ -rays from blazars. The joint neutrino⁶⁵ and EM detection^{66–68} of the flaring blazar TXS 0506+056 was an exciting result, being the first time that a known source was shown to be associated (albeit only at the $\sim 3\sigma$ level) with a high-significance astrophysical high-energy neutrino (FIG. 2).

Blazars are AGN, galaxies with a massive central black hole powering a relativistic jet outflow pointing close to the observer line of sight. They are classified into BL Lac objects (highly variable, extragalactic AGN) and flat spectrum radio-quasars. TXS 0506+056 appears to be of the former type although there are also arguments for it being of the latter⁶⁹. Blazars are notorious for exhibiting sporadic and intense γ -ray-flaring episodes, one of which was in progress at the time the track-type neutrino was observed from the blazar. A further analysis indicated that other neutrinos may have been associated with this source before⁷⁰. This provided valuable constraints on the radiation mechanisms and the sources of the diffuse HEN background. Based on simple one-zone emission models in which both HENs and γ -rays originate from the same region, the detection

Short GRB

A short gamma-ray burst, confirmed recently to be due to the merger of a binary neutron star; also expected from neutron star–black hole binary mergers.

r-Process

The abbreviation of 'rapid neutron capture nuclear process', whereby a nucleus rapidly increases its atomic number by repeatedly capturing neutrons.

Table 1 | **Plausible target detector sensitivities**

Stage	LIGO BNS	LIGO BBH	Virgo BNS	Virgo BBH	KAGRA BNS	KAGRA BBH
Early	40–80	415–775	20–65	220–615	8–25	80–250
Mid	80–120	775–1,110	65–85	615–790	25–40	250–405
Late	120–170	1,110–1,490	65–115	610–1,030	40–140	405–1,270
Design	190	1,640	125	1,130	140	1,270

Target detector sensitivities in Mpc give the average detection distance (range in Mpc), giving the average detection distance (range) at which a $2 \times 1.4 M_{\odot}$ binary neutron star (BNS) merger and $2 \times 30 M_{\odot}$ (M_{\odot} is the solar mass) binary black hole (BBH) merger may be detected with the Laser Interferometer Gravitational-Wave Observatory (LIGO), Virgo and the Kamioka Gravitational Wave Detector (KAGRA). From REF.¹⁴¹, CC-BY-4.0 (<https://creativecommons.org/licenses/by/4.0/>).

of a neutrino is a low-probability event^{67,71,72}. Based on a stacking analysis of HENs and blazars, it appears that the blazar population as a whole may account for ~10–30% of the entire IceCube neutrino background⁷³, so other sources may in any case need to explain the bulk of the neutrino background.

Emerging questions and challenges

Missing counterparts

With 12 BBH mergers detected in GWs (FIG. 2) as of July 2019, the lack of EM and HEN counterparts of BBH mergers is frustrating. Such EM and HEN emissions are expected to be faint at best in BBHs (see, for example, REFS^{74,75}), but they would be very useful for a better understanding of the binary origin and environment, and to obtain an improved localization compared with GWs (see, for example, REFS^{75–78}). A much larger sample of BBHs will be needed, extending to both smaller and larger masses, to test the hypothesis that BBHs provide a cosmologically important dark matter component (see REFS^{79–81}).

HENs from binary neutron stars. HENs originating from binary neutron stars would provide an example of a ‘triple messenger’ source, and would clarify important open questions regarding these objects. Possible signals and observing strategies have been discussed in REFS^{78,82,83}. Expected HEN fluxes are low, especially for off-axis jet viewing^{84,85}, but in the best case they may be marginally detectable by IceCube (or more likely, by a future IceCube Generation 2 (IceCube-Gen2)), and would greatly help clarify the physics of the relativistic jet and the larger-angle slower outflows that give rise to the GRB, the afterglow and the kilonova emission of these mergers.

HEN flares in blazars

A confirmation of HEN flares in blazars could be established through additional observations of TXS 0506+056 and other AGN. This is urgently needed to address the origin of the IceCube background and establish any possible connection between the HEN and UHECR backgrounds. Progress in these studies will also require more targeted calculations of AGN neutrino production models, yielding detailed predictions for X-ray, γ-ray, optical and radio constraints. The stacking analyses of blazar EM flares against observed HENs^{73,86} and theoretical arguments⁸⁷ suggest that other sources than blazars must provide the dominant contribution to the HEN background, and observational correlation studies involving alternative source candidates are needed⁴¹.

Masses and spins of compact mergers

The compact mergers detected using GWs raise new questions, for example, regarding the origin, formation and evolution of the ‘heavy’ binary stellar black holes (~30 M_{\odot} , where M_{\odot} is the solar mass). Another question is why do the LIGO/Virgo black holes have very low spins or spins misaligned with the orbital angular momentum. This is in contrast to other (non-merging) black hole candidates detected previously in X-rays only, some of which have very large spins. In addition, the ultimate fate of the binary neutron star merger GW 170817 is unknown: how long did the remnant last before turning into a black hole, if it finally ever did? These and related questions are discussed in REFS^{27,88}. Future GWs observations could provide answers.

Reducing UHECR uncertainties

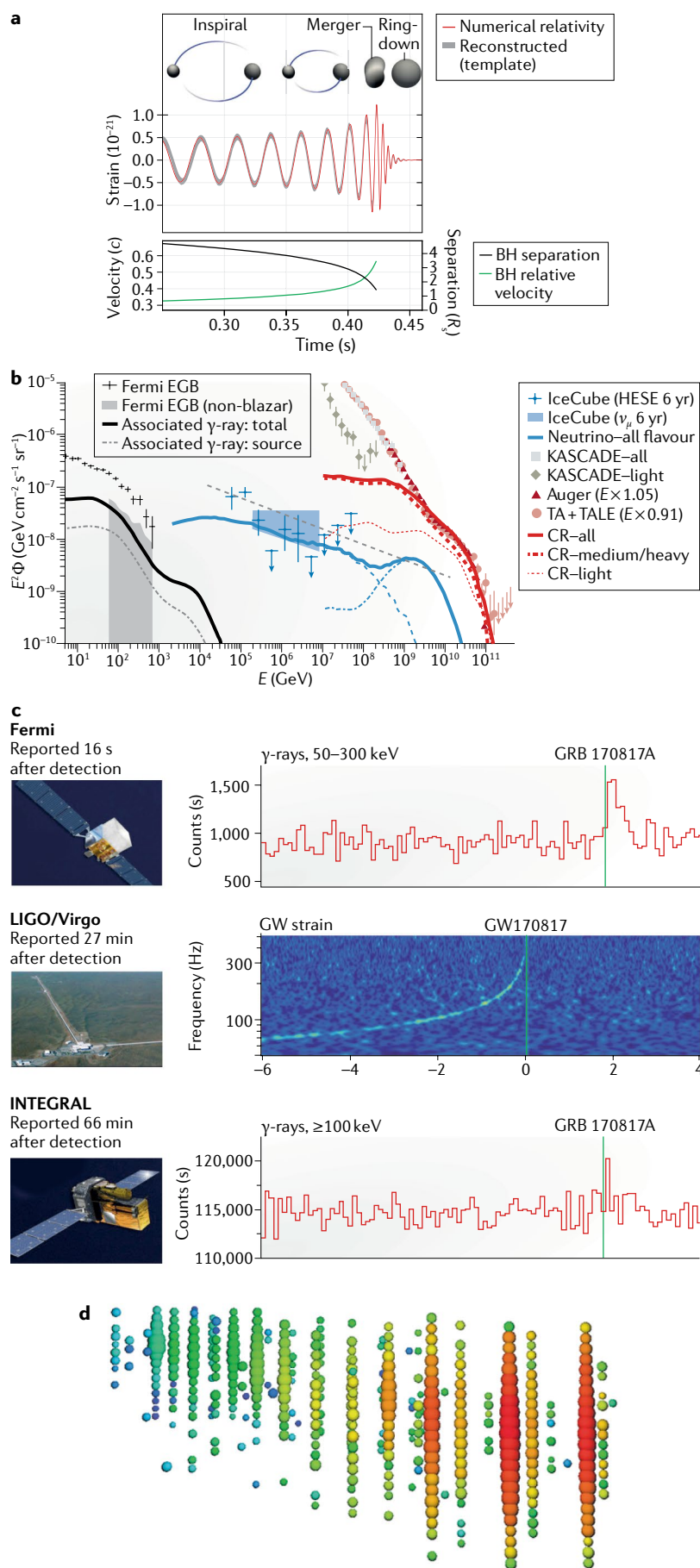
The UHECR arrival direction uncertainties are large and UHECR arrival times are delayed by ~10⁴–10⁵ years relative to any simultaneously produced EM or neutrino emission, so direct correlation attempts have been made against only quasi-steady, non-bursting sources, but have, so far, been unsuccessful^{89,90}. At the highest energies, UHECR positional correlations with muon neutrino tracks, UHE neutrinos and/or γ-rays could lead to a better pinpointing of the sources. This will require much better instruments and more sensitive neutrino/EM correlation analyses as well as much more detailed production models for likely source candidates.

Improved correlation measurements

Statistically significant measurements of the correlations (or lack thereof) between UHECR, HEN, GW and EM messengers are urgently needed, and it is also necessary to explain the UHECR spectrum and chemical composition with an appropriate distribution of specific sources^{91,92}. Observations must be carefully fitted to model predictions of potential candidates (such as AGN, GRBs, tidal disruption events, clusters of galaxies and so on) and more sophisticated models must be computed, and tested against the observed diffuse neutrino and γ-ray backgrounds.

Theory and simulation

As far as UHECR, HEN and GW sources are concerned, theory and simulations are still in their infancy. Although the HEN–EM interrelation is in principle straightforward (aside from nonlinearities introduced by EM and hadronic cascades), an understanding of their interrelations with UHECRs is complicated by the fact



that the latter are charged, and hence travel in intricate paths, depending on the magnetic fields⁹³. In addition, at energies above $\sim 10^{17}$ – 10^{18} eV, their cross-sections have higher uncertainties. For BBH and binary neutron star mergers, significant progress is urgently required to understand the post-merger dynamics, the final state of the remnant, the physics of the ejecta and how black hole–neutron star mergers differ from binary neutron star mergers⁹⁴. Core-collapse supernova simulations are also challenging^{95,96}, in particular, the lack of reliable GW waveforms necessitates relying on suboptimal techniques for attempting their GW detection, making it far more difficult to distinguish between different collapse models/scenarios.

Improving sensitivities

The ultrahigh-energy neutrino range 10^{17} – 10^{20} eV measurements by ANITA²³ and other future experiments need to achieve at least an order of magnitude greater sensitivity to probe the cosmogenic neutrino background. The physical picture is complicated by the UHECRs interacting with the cosmic photon backgrounds, and the degeneracies induced by the effect of the UHECR source luminosity function and redshift distance distribution, combined with the cosmic ray chemical composition uncertainties^{97–99}. The ANITA anomalous upward-going events¹⁰⁰, if confirmed, could provide clues about cosmic tau neutrinos, or perhaps beyond-the-standard-model physics. Agreement between the ANITA, IceCube and Pierre Auger Observatory measurements will need to be carried out, together with significantly more detailed theoretical investigations^{101–104}.

Fig. 2 | Examples of recent cosmic multi-messenger advances involving the electromagnetic, weak, gravitational and strong forces. **a** | The first gravitational wave (GW) detection from Laser Interferometer Gravitational-Wave Observatory (LIGO)/Virgo of the GW150914 binary black hole (BH) merger⁴, showing the inspiral, merger and ringdown phases the theoretical and measured waveform, the separation and the relative velocity. **b** | The interrelation expected between (from left to right) the energy spectrum of the diffuse backgrounds in γ -rays, high-energy neutrinos and ultrahigh-energy cosmic rays (CR), based on a black hole jet source model⁴⁰ (here E is particle energy, and Φ is flux per unit area, time and solid angle; the measurements are from the KASCADE-Grande, Telescope Array (TA) and Telescope Array Low Energy extension (TALE), Pierre Auger Observatory, IceCube and Fermi Gamma-Ray Space Telescope; EGB stands for extragalactic gamma-ray background and the dashed grey line corresponds to the calculations from REF.⁴⁰). **c** | LIGO, Virgo and Fermi simultaneous multi-messenger discovery of the binary neutron star merger GW/GRB 170817. **d** | Light track of the muon produced by a 290 TeV muon neutrino coming from the direction of the blazar TXS 0506+056, detected on 22 September 2017 by IceCube. Panel **a** is reproduced from REF.⁴, CC-BY-3.0 (<https://creativecommons.org/licenses/by/3.0/>); panel **b** is reproduced from REF.⁴⁰, Springer Nature Limited; panel **c** is reproduced with permission from NASA's Goddard Space Flight Center, Caltech/MIT/LIGO Lab and ESA; panel **d** is reproduced with permission from the IceCube Collaboration.

New instruments and expected results

The spectacular results achieved by combining observations from different instruments (BOX 3) opened wide new vistas in high-energy astrophysics. This motivated the **development of more sophisticated and more powerful experiments and missions** (see BOX 3 for upcoming and planned facilities), whose goal is to answer some of the key new questions listed in the previous section.

EM detectors

Among the major space-based EM facilities coming online within the next 5–10 years is the Chinese-French **Space Variable Object Monitor¹⁰⁵ (SVOM; FIG. 3a)**, **designed for detecting γ -ray, X-ray and optical transients and scheduled for launch in late 2022**. Two other Chinese missions are in preparation: the Electromagnetic Counterpart All-sky Monitor (GECAM)¹⁰⁶, with an all-sky coverage aimed at detecting GW counterparts in the 6 keV to 5 MeV energy range, scheduled for the mid-2020s; and the time-domain Explorer-class Einstein Probe¹⁰⁷, with a 3,600 deg² field-of-view sensitivity at 0.5–5.0 keV, planned for the end of 2022. An Israeli–US mission called Ultraviolet Transient Astronomy Satellite (**ULTRASAT¹⁰⁸**) **has been proposed, with an ultraviolet (250–280 nm), fast-slewing (~minutes) imaging detector of 250 deg² field of view, which could detect hundreds of supernovae, ~10 binary neutron star counterparts per year and ~100 tidal disruption events per year.**

argumentos de peso
There is a strong case for an X-ray– γ -ray satellite **to provide real-time triggers and data**, which would be critical for multi-messenger studies. A possible NASA mission that recently completed its Phase A study is the International Space Station Transient Astrophysics Observer (**ISS-TAO¹⁰⁹**), with a γ -ray transient monitor and wide-field (350 deg²) X-ray imager, **whose prime target would be EM counterparts of GW sources. This mission would be launched by 2032.**

A significant role in detecting or confirming transients of multi-messenger importance will be played by the Zwicky Transient Facility (ZTF)¹¹⁰ and the All-Sky Automated Survey for Supernovae (ASAS-SN) facility¹¹¹. In the 5–10 year time frame, the multi-national Cherenkov Telescope Array (CTA)¹¹² (FIG. 3b) and the Chinese Large High Altitude Air Shower Observatory¹¹³ (LHAASO) ground-based facilities will survey the sky at TeV–PeV γ -ray energies³⁰. Both facilities use the air Cherenkov technique, but whereas CTA includes steerable dishes that provide good angular localization, useful for point sources, LHAASO largely observes as the sky moves by, similarly to HAWC, which works better for extended or diffuse emission. A major optical/infrared survey facility instrument is the Large Spectroscopic Survey Telescope¹¹⁴ (LSST), whereas the Square Kilometer Array¹¹⁵ (SKA) will provide milli-arcsecond spatial resolution images at radio frequencies. Other telescopes in preparation are the ground-based optical/infrared Thirty Meter Telescope, the Extremely Large Telescope and the Giant Magellan Telescope^{116–118}.

For the early 2030s, the European Space Agency (ESA) is preparing a major flagship X-ray mission named Advanced Telescope for High-ENergy Astrophysics (ATHENA)¹¹⁹, which will trace the galaxy formation and

metallicity evolution of the Universe with its large-area detectors, and can study Population III GRBs. Pending a final ESA selection in 2022 and planned for a launch in 2032 is the smaller, but nimbler, fast-slewing (~minute) satellite Transient High-Energy Sky and Early Universe Surveyor (THESEUS)¹²⁰, designed to discover long GRBs at redshifts $z \approx 9$ and seek binary neutron stars counterparts with a soft X-ray imager, an X- and γ -ray spectroscopic imager and an 0.7 m class infrared telescope, which will also provide triggers for ATHENA. The NASA All-sky Medium Energy Gamma-ray Observatory (AMEGO) satellite¹²¹, sensitive to γ -rays from 0.2 MeV to ~10 GeV and the German mission¹²² extended Roentgen Survey (eROSITA) 0.3–10 keV space detector will play important roles in X- and γ -ray astronomy, as well as in the EM detection of hidden neutrino sources.

To complement the above large facilities, it is extremely important to also have various fast, large field-of-view robotic ground-based telescope systems that can follow-up transient candidates within seconds after an alert is triggered.

High-energy and low-energy neutrino detectors

HEN detector planned **upgrades include the IceCube High Energy Array and the denser Precision IceCube Next Generation Upgrade (PINGU) subarray**, as part of an extended (10 Gt) IceCube-Gen2 (see REF.¹²³ and FIG. 3). In the Northern Hemisphere, the completion of the Cubic Kilometre Neutrino Telescope (KM3NeT) 3–4 Gt detector¹²⁴ in the Mediterranean Sea is expected by 2026 (FIG. 3). The localization angular error box improvements for muon tracks are expected to lead to 0.3–0.5° uncertainties. **The relative advantages/disadvantages of ice compared with water as a Cherenkov detector medium are that the light absorption length in ice is ~100 m versus ~15 m for clear ocean water and the scattering length for ice is ~20 m whereas it is ~100 m for water.** In addition, ocean water contains radioactive ⁴⁰K, affecting the energy resolution signal-to-noise ratio. **These lead to a relative better/worse energy resolution, and worse/better angular resolution in ice and water, respectively^{123,124}.**

Another gigaton water-based neutrino detector¹²⁵, the Baikal Gigaton Volume Detector (Baikal-GVD), in Lake Baikal, Russia, is planned for 2021–2022. It aims to identify large-scale anisotropies and individual sources with neutrinos only, or in tandem with other multi-messengers. **Combined observations with these facilities will enable the use of doublets and multiplets (the statistically expected frequency of two or more neutrinos observed within a certain angular and time window) for source population studies, and will increase the prospects of identifying galactic sources, reliably identify tau neutrinos and determine the flavour composition of the HEN background.**

The **Hyper-Kamiokande (Hyper-K)** next-generation megaton water Cherenkov detector¹²⁶, operating at MeV to GeV energies, is located in the Kamioka mine in Japan and is scheduled to begin construction in 2020. **It will be an order of magnitude larger than its predecessor Super-Kamiokande**, in which the addition of gadolinium to the water is providing significantly improved sensitivity. Hyper-K **will be able to detect individual supernova**

Box 3 | Current, upcoming and proposed multi-messenger astronomy instruments for different messengers

Electromagnetic

• Current

- Swift satellite: BAT 15–150 keV; XRT 0.2–10 keV; UVOT 170–560 nm
- Fermi satellite: LAT 20 MeV–300 GeV; GBM 10 keV–25 MeV
- HAWC (north ground air shower array): 0.3–100 TeV
- MAGIC, HESS, VERITAS ground IACTs: 150 GeV–30 TeV
- ZTF, ASAS-SN ground surveys, optical, near-IR
- LOFAR: ground array transient survey, radio

• In construction

- SVOM satellite (~2021): GRM 30 keV–5 MeV, ECL AIRS 4–250 keV; VT 400–950 nm
- GLOWBUG, space-ISS (~2023): scintillator array, 30 keV–5 MeV
- Einstein Probe satellite (late 2022): large FoV, 0.5–5 keV time-domain explorer
- GECAM satellite (mid-2020s) all-sky, 6 keV–5 MeV, GW counterpart
- eROSITA, satellite (~2020): all-sky transient survey, 0.3–10 keV
- LHAASO ground air shower array (~2022) 100 GeV–1 PeV
- LSST ground survey (~2022) optical, near-IR
- SKA ground array survey (~2022) radio interferometer
- CTA ground IACT arrays, (2025?): 4 LST 20–150 GeV, 40 MST 0.15–5 TeV, 70 SST 5–300 TeV

• Proposed

- ISS-TAO, space-ISS (~2023?): GTM 10 keV–1 MeV
- ULTRASAT satellite (~2023?): 50 cm UV telescope, 250–280 nm
- AMEGO satellite (~2030s?): 300 keV–10 GeV
- HAWC-Southern Hemisphere (~2030s?): 4 × north size, higher altitude, 0.1–100 TeV
- TMT, ELT, GMT (~2025–2030) 30 m class optical/IR ground-based telescopes

High-energy neutrinos

• Current

- IceCube ice Cherenkov array: Gt array TeV–100 PeV, Deep Core array 10–300 GeV
- ANTARES water Cherenkov array: 50 Mt, TeV–10 PeV
- Super-K water Cherenkov array: 50 kt, 4.5 MeV–1 TeV
- ANITA balloon radio detector: 10^{17} – 10^{20} eV

• In construction

- IceCube upgrade (~2021): PINGU 7 new strings, 5–20 GeV
- KM3NeT water Cherenkov array (~2024?) 4–5 Gt TeV–10 PeV, ORCA 1–20 GeV, ARCA 0.1 TeV–100 PeV
- Baikal-GVD water Cherenkov array (~2024?) 2 Gt, 5 TeV–10 PeV
- Hyper-K water Cherenkov array (~2026) 1 Mt, 1 MeV–1 TeV

• Proposed

- IceCube-Gen2 (~2030s?): PINGU 1–20 GeV, high-energy extension <100 PeV

- ARIANNA ice radio array (~2025–2030s?): 10^{17} – 10^{20} eV
- ARA/RNO ice radio array (~2025–2030s?): 10^{17} – 10^{20} eV
- GRAND ground detector array (~2030s?): 10^{17} – 10^{21} eV

Ultra-high energy cosmic rays

• Current

- Auger extensive air shower array: 3,000 km², 1,600 tanks, 27 air fluorescence telescopes, 10^{17} – 10^{21} eV
- TA extensive air shower array: 760 km² surface tanks + air fluorescence telescope, 10^{17} – 10^{21} eV

• In construction

- AugerPrime: add 1,600 surface scintillators, 10^{17} – 10^{21} eV
- LHAASO ground air shower array (~2023?) 100 GeV–1 PeV
- TAx4 (4 times previous area ~3,000 km²), (~2023?): 10^{17} – 10^{21} eV

• Proposed

- K-EUSO, space-ISS (~2023–25?): UV telescope detector of extensive air showers 10^{17} – 10^{21} eV
- POEMMA satellite array (~2030s?): UV telescope detector, 10^{17} – 10^{20} eV
- GRAND ground detection array (~2030s?): 10^{17} – 10^{21} eV
- TRINITY ground radio array (~2030s?): UV telescope detector, $10^{16.5}$ – 10^{18} eV

Gravitational waves

• Current

- LIGO, 2 × 4 km GW ground interferometer: ~ 10 – 10^3 Hz (~1–100 M_{\odot} equal mass binaries)
- Virgo 2 × 3 km GW ground interferometer: ~ 10 – 10^3 Hz (~1–100 M_{\odot} equal mass binaries)
- Pulsar timing array radio interferometer, PTA, NANOGrav: (10^5 – 10^7 M_{\odot} equal mass binaries)

• In construction

- LIGO, A+ upgrade (2023): (double previous detection distance)
- KAGRA 2 × 3 km GW underground interferometer (~2022): ~ 10 – 10^3 Hz (~1–100 M_{\odot} equal mass binaries)
- LIGO-India 2 × 4 km GW ground interferometer (~2024): ~ 10 – 10^3 Hz (~1–100 M_{\odot} equal mass binaries)
- Pulsar timing array radio interferometer (>2020), PPTA, EPTA: (10^5 – 10^7 M_{\odot} equal mass binaries)
- eLISA, 3 × 2.5 × 10⁶ km (~2030 s) GW space interferometer: ~ 10^{-4} – 10^{-1} Hz (~ 10^5 – 10^7 M_{\odot} equal mass binaries)

• Proposed

- LIGO Voyager upgrade (~mid-2020s) (BNS range up to 700–1,000 Mpc)
- Cosmic Explorer, 2 × 40 km (~2030s) GW ground interferometer: ~ 10 – 10^3 Hz (~1–100 M_{\odot} equal mass binaries)
- Einstein Telescope, 3 × 10 km (~2030s) GW underground interferometer: ~ 10 – 10^3 Hz (~1–100 M_{\odot} equal mass binaries)

ANITA, Antarctic Impulsive Transient Antenna; ANTARES, Astronomy with a Neutrino Telescope and Abyss environmental REsearch; AMEGO, All-sky Medium Energy Gamma-ray Observatory; ARA, Askaryan Radio Array; ARIANNA, Antarctic Ross Ice-Shelf ANTenna Neutrino Array; ASAS-SN, All-Sky Automated Survey for Supernovae; BAT, burst alert telescope; CTA, Cherenkov Telescope Array; ELT, Extremely Large Telescope; FoV, field of vision; GECAM, Electromagnetic Counterpart All-sky Monitor; GMT, Giant Magellan Telescope; GRAND, Giant Radio Array for Neutrino Detection; GBM, Gamma-ray Burst Monitor; GRM, Gamma Ray Monitor; HAWC, High Altitude Water Cherenkov Observatory; HESS, High Energy Stereoscopic System; IACT, imaging atmospheric Cherenkov telescope; IR, infrared; ISS-TAO, International Space Station Transient Astrophysics Observer; KM3NeT, Cubic Kilometre Neutrino Telescope; LAT, Large Area Telescope; LHAASO, Large High Altitude Air Shower Observatory; LOFAR, Low Frequency Radio Array; LSST, Large Spectroscopic Survey Telescope; LST, Large Survey Telescope; MAGIC, Major Atmospheric Gamma Imaging Cherenkov Telescopes; MST, Medium Survey Telescope; RNO, Radio Neutrino Observatory; SKA, Square Kilometer Array; SVOM, Space Variable Object Monitor; UVOT, ultraviolet/optical telescope; VERITAS, Very Energetic Radiation Imaging Telescope Array System; XRT, X-ray telescope; ZTF, Zwicky Transient Facility; BNS, binary neutron star; eLISA, evolved Laser Interferometer Space Antenna; EPTA, European Pulsar Timing Array; GRAND, Giant Radio Array for Neutrino Detection; KAGRA, Kamioka Gravitational Wave Detector; LHAASO, Large High Altitude Air Shower Observatory; LIGO, Laser Interferometer Gravitational-Wave Observatory; M_{\odot} , solar mass; NANOGrav, North American Nanohertz Observatory for Gravitational Waves; POEMMA, Probe Of Extreme Multi-Messenger Astrophysics; PPTA, Parkes Pulsar Timing Array; PTA, pulsar timing array; SST, Small Survey Telescope; TA, Telescope Array; TMT, Thirty Meter Telescope; ULTRASAT, Ultraviolet Transient Astronomy Satellite; UV, ultraviolet. VT, Visual Telescope.

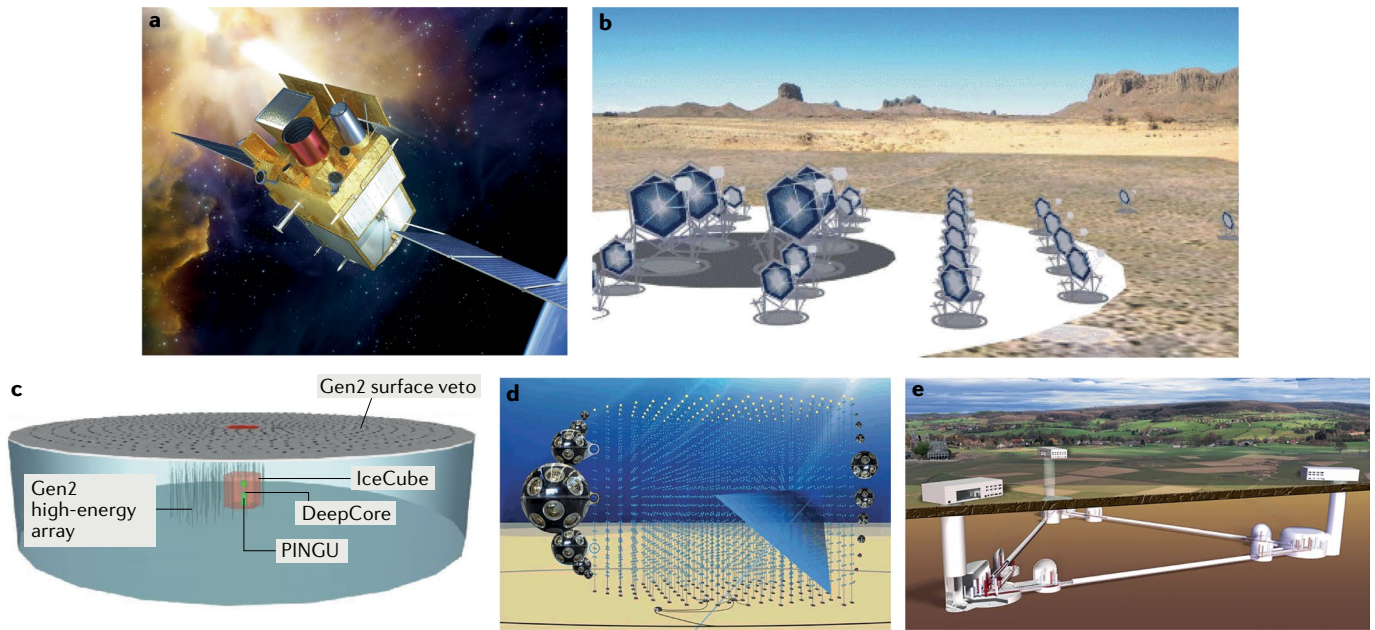


Fig. 3 | Examples of new detectors in the planning stage. **a** | The Space Variable Object Monitor (SVOM) China–France γ -ray burst multi-wavelength follow-up satellite, expected in 2022 (REF.¹⁰⁵). **b** | Schematic of the Cherenkov Telescope Array (CTA) γ -ray ground array, expected in 2024 (REF.¹⁶⁵). **c** | IceCube Generation 2 (IceCube-Gen2), including current IceCube and DeepCore, and the planned high-energy array, super-dense Precision IceCube Next Generation Upgrade (PINGU) subarray and extended surface array (larger Askaryan Radio Array radio array not shown)¹²³. **d** | The Cubic Kilometre Neutrino Telescope (KM3NeT) planned

3–4 km³ neutrino detector in the Mediterranean Sea, which will include also the high-energy Astroparticle Research with Cosmics in the Abyss (ARCA) and low-energy Oscillation Research with Cosmics in the Abyss (ORCA) subarrays¹²⁴. **e** | Schematic of the planned European Union next-generation Einstein gravitational wave interferometer¹⁴³. Panel **a** is reproduced with permission from CNES/Oliver Sattler 2015; panel **b** is reproduced from REF.¹⁶⁶, Springer Nature Limited; panel **c** is reproduced from REF.¹⁶⁷, Springer Nature Limited; panel **d** is reproduced courtesy of the KM3NeT consortium; panel **e** is reproduced courtesy of the ET design study team.

explosions out to ~ 4 Mpc, roughly one every 3–4 years, and in 10–20 years it could measure the relic supernova diffuse neutrino flux in the 16–30 MeV energy range¹²⁷.

At the highest energies, 10^{17} – 10^{21} eV, the ANITA balloon experiment²³ will undergo further sensitivity improvements in the coming years. On a longer time-scale (2022–2032), much larger ground-based detectors are expected. These would be using the Askaryan radio technique for detecting neutrinos and UHECRs in the same 10^{17} – 10^{21} eV range, and include the Antarctic Ross Ice Shelf ANTenna Neutrino Array (ARIANNA)¹²⁸ and the Askaryan Radio Array (ARA)¹²⁹, or possibly a combination of these efforts, the Radio Neutrino Observatory (RNO)/ARA. These facilities are aimed at detecting the cosmogenic neutrino background component produced by GZK UHECRs, and probing more deeply the nature of the steepening of the UHECR spectrum beyond 10^{20} eV. Other large-scale detector proposals with this goal are the Chinese-led Giant Radio Array for Neutrino Detection (GRAND) 10,000 km² array planned for the 2025 to 2030s¹³⁰ and the Probe Of Extreme Multi-Messenger Astrophysics (POEMMA)¹³¹ and Trinity¹³² projects.

UHECR detectors

UHECR facilities undergoing major upgrades include the AugerPrime addition of 1,600 surface scintillation detectors on top of the existing water Cherenkov tanks of the Pierre Auger Observatory and updated electronics¹³³, and the Telescope Array upgrade to the TAx4

configuration, a fourfold surface enlargement¹³⁴. In the next 5–10 years, the planned KLYPVE Extreme Universe Space Observatory (K-EUSO) experiment¹³⁵ on the ISS could achieve uniform exposure across the Southern and Northern hemispheres of 4×10^4 km² sry, an order of magnitude larger than AugerPrime or TAx4. Radio observations with the Low Frequency Radio Array (LOFAR)¹³⁶ should also contribute substantially to an improved understanding of UHECRs.

In the lower energy range of 10^{12} to $>10^{15}$ eV, the ISS-CREAM instrument¹³⁷ on the ISS (building on the earlier Cosmic Ray Energetics And Mass (CREAM) balloon flights) and the future Chinese mission¹³⁸ High Energy cosmic Radiation Detection facility (HERD), could uncover the spectrum and compositions of cosmic ray nuclei with charges in the $Z = 1$ –26 range.

In the next 10–15 years, the planned POEMMA satellites¹³¹ are expected to achieve an increase in the exposure by 100 times while the planned Fluorescence detector Array of Single-pixel Telescopes (FAST) ground array¹³⁹ would provide 10 times the exposure with high-quality events. These advances will address the chemical composition and anisotropy issues of UHECR, clarify the interpretation of the surmised three cosmic ray components making up the entire spectrum¹⁴⁰, determine the maximum energy of galactic cosmic rays, and probe in more detail the nature of the spectral cut-off, the transition from galactic to extragalactic components, the strength of the galactic and intergalactic magnetic fields and so on.

Air shower array
An array of detectors measuring the secondary particles or photons produced by a primary cosmic ray hitting Earth's atmosphere.

Improved and new GW detectors

The upgrades of LIGO and Virgo are continuing¹⁴¹, and they will reduce the 90% median angular error box size for source identifications down to 120–180 deg² (with 12–21% with ≤ 20 deg²) by the 2019-onward third operating run. The Japanese Kamioka Gravitational Wave Detector (KAGRA) detector being built in the Kamioka mine in Japan is expected to reach a sensitivity comparable to Advanced LIGO and Advanced Virgo by 2024. A new LIGO observatory is under construction in India to house a third detector (LIGO-India). With these additional facilities, the expected median 90% localization error box sizes will be 9–12 deg². The number of expected BBH and neutron star detections and the limiting distances are summarized in TABLE 1.

Among the next generation of ground-based GW detectors planned for the 2020–2030s¹⁴², the ‘A+’ upgrade to the LIGO facilities has been approved. It should provide a further factor of two increase in detection range beyond the detectors’ advanced sensitivity. A further upgrade, termed LIGO Voyager, would have a new detector operating in the existing LIGO, with cryogenic mirrors in the existing LIGO vacuum envelope. This could bring a further factor of three increase in the binary neutron star detection range (to 1,100 Mpc), with a low-frequency cut-off down to 10 Hz.

In the European Union, the planned underground Einstein Telescope¹⁴³ (FIG. 3), with three 10-km-long arms, will be able to measure the GW polarization of BBHs and binary neutron star sources from distances 3 to 10 times farther than with the current design sensitivity of the LIGO/Virgo designs. Further in the future, in the United States, the Cosmic Explorer ground-based observatory¹⁴⁴ would use 40 km arms to achieve another order of magnitude improvement in sensitivity over the 10 Hz to 10⁴ Hz frequency range and detect compact binary in-spirals throughout our Hubble volume.

To study the merger of the much larger (10^6 – $10^8 M_{\odot}$) supermassive black holes located at the centre of galaxies, the European Union is planning a large space-based GW detector called the evolved Laser Interferometer Space Antenna (eLISA)¹⁴⁵, consisting of an interferometer using three small satellites in solar orbit. A different technique for the exploration of supermassive black hole mergers is provided by the pulsar timing arrays (PTAs)¹⁴⁶, such as the North American Nanohertz Observatory for Gravitational Waves (NANOGrav), Parkes Pulsar Timing Array (PPTA) and European Pulsar Timing Array (EPTA)^{147,148}. This technique relies on measuring the time delays in the EM radio signals from distant pulsars caused by the spacetime variations induced by the GW field produced by merging black hole binaries, and is expected to yield the first stochastic (population-integrated) detections in the near future.

The multi-messenger synergy

The Astrophysical Multi-messenger Observatory Network (AMON)¹⁴⁹ is a multi-institution consortium that has signed agreements with a number of observatories using different messengers. The main aim is to combine disparate rare signals appearing in coincidence, so that even subthreshold detections in one messenger,

when combined with other subthreshold signals in other messengers, can yield a reliable above-threshold detection. Another aim is to rapidly distribute interesting transient alerts arising from any observatory to all the other observatories and the community, to facilitate rapid follow-up. The architecture of AMON consists of a central hub connected to individual observatories, from which it receives individual sub-threshold and above-threshold alerts, which are then subject to analysis and/or are redistributed to other observatories. This greatly increases the speed and effectiveness of reaction to a trigger, compared with the large number of traditional individual observatory-to-observatory connections. Observatories that have signed up to the AMON network include, so far, ANTARES, Pierre Auger Observatory, Fermi-LAT, Fermi-GBM, HAWC, IceCube, Swift-BAT, VERITAS and others. Live data streams from IceCube, HAWC, Fermi and Swift are currently being received by AMON, triggering alerts as in the 0506+056 blazar neutrino and γ -ray flare discovery^{67,150}, and other coincident subthreshold analyses are being carried out, for example, for LIGO and Swift-BAT, HAWC and others. The unique and most promising feature of AMON is its emphasis on leveraging multiple live subthreshold alerts. In addition, subthreshold analyses are also being carried out using archival data from different individual observatories¹⁵¹. Other groups are also developing algorithms and strategies for multi-messenger searches¹⁵².

Theory and simulations

The high-quality data provided by the facilities outlined above will only yield fruit insofar as it is thoroughly analysed and interpreted through realistic multi-messenger astrophysical source models (while keeping in mind the possibility of physics beyond the standard model). Such models must be considered at three levels. The basic level operates on the overall conceptual picture, using analytical or semi-analytical descriptions including the source geometry, composition, dynamics and multi-messenger radiation properties (see REFS^{19,41,42,44,87,141,153,154} for reviews). The second level involves detailed numerical simulations of the dynamics of the formation of the sources and their evolution leading to the state at which the various types of multi-messenger emissions occur^{155–158}. The third level involves detailed calculations and simulations of the radiation physics, using large-scale numerical codes to describe the emission of multi-messengers, followed by their possible changes during propagation from the source to the observer, and their specific effects on particular types of detectors^{40,92,149,159–161}. At all three levels, for low source numbers or low signal rates, diffuse backgrounds must be calculated using simulated source signals convolved over cosmological luminosity and redshift distributions⁹².

All these three types of calculations will have to be considerably expanded and refined to address and exploit the potential of the much more detailed data expected from the new facilities. Even for the semi-analytical studies, the increasing sensitivity and range of the detectors will make it necessary to use farther-reaching and fainter-reaching source luminosity functions, more extensive redshift and mass distributions,

Supermassive black holes
A black hole in the range 10^5 to $10^{10} M_{\odot}$, usually at the centre of a galaxy.

intervening plasma and radiation field spectral densities, and so on. The source formation and dynamics studies, which are increasingly incorporating general relativistic and magnetohydrodynamic effects, will need to be extended to the 3D regime more often than before, and the use of adaptive mesh and shock capture methods^{94–96} will have to be exploited and developed further. There will be an increasing need for a better cross-calibration of the various Monte Carlo methods used in simulating high-energy particle interactions and cascades, incorporating the errors due to theoretical uncertainties, especially in the extrapolation to energies beyond those of laboratory particle accelerators. The atomic and nuclear physics of very heavy elements is poorly understood and sparsely studied in the laboratory, yet to reliably elucidate the sources of the r-process elements in the Universe (lately ascribed largely to binary neutron star mergers), the error estimates arising from these theoretical and experimental laboratory uncertainties will need to be quantified and taken into account.

Outlook

Some of the most important issues that will be addressed in the next 5–10 years with upgraded GW detectors such as LIGO, Virgo and KAGRA, as they improve sensitivity at frequencies above 0.1 kHz, are the detailed exploration of the lower mass range of BBH mergers, testing whether the final outcome of neutron star mergers is a massive neutron star or a black hole, probing the final ringdown of spacetime around a newly formed black hole, determining the maximum mass of neutron stars, further testing whether general relativity remains valid under extreme density and pressure conditions, and exploring the nature of the central mechanism of GRBs. As GW detectors push towards lower frequencies, below 10 Hz, it will be possible to probe intermediate mass black holes of 100–500 M_{\odot} , important for understanding how the most massive black holes at the centre of galaxies form. To obtain more reliable results, larger interferometer arm lengths such as the ~10 km ones of the Einstein Telescope or 40 km of the Cosmic Explorer experiments will be needed. On the 10–20 year timescale, even longer arms, such as the 2.5-million-km arms of the space-based eLISA interferometer, will measure frequencies below ~0.1 Hz that can probe the merger of ~ $10^6 M_{\odot}$ black hole mergers, important for understanding the growth of galaxies and clusters of galaxies in the Universe, and the existence of a primordial GW background left over from the inflationary era of the early Big Bang.

The neutrino detector upgrades such as PINGU in IceCube and ORCA in KM3NeT will provide better statistics in the 1–10 GeV energy range to probe fundamental neutrino physics issues such as the hierarchy of the mass ordering, and the mixing angles between flavours, constraining the neutrino masses and checking for the existence of sterile neutrinos. These problems are likely to be resolved in the next 5–10 years with the help of these and other detectors. The next-generation IceCube-Gen2 is likely to identify the sources from which HENs originate⁴¹. In the Northern Hemisphere, the KM3NeT detector will be able to observe HENs

from our Galactic Centre, where most of the (so far undetected) galactic neutrino sources reside.

The upgraded ANITA balloons and, if funded, the ARIANNA and RNO/ARA experiments in Antarctica will make progress towards detecting the 10^{17} – 10^{19} eV cosmogenic neutrinos produced by UHECR protons interacting with the cosmic microwave background, or by UHECR nuclei interacting with the diffuse starlight. These experiments will also complement IceCube-Gen2 in the pursuit of identifying tau neutrinos. More reliable determinations may need to wait for larger experiments such as GRAND and POEMMA, which will also address the chemical composition of the highest energy UHECRs.

The next galactic supernova should be an ideal and important event for multi-messenger astrophysics, which can be studied by the Hyper-K¹²⁶ and the Jiangmen Underground Neutrino Observatory (JUNO)¹⁶² experiments to address fundamental issues of neutrino oscillations and supernova physics^{163,164}.

The next upgrades of the Pierre Auger Observatory and the Telescope Array UHECR arrays are expected to answer the question of the chemical composition of UHECRs independently of the clues from the above neutrino detectors, providing a much needed consistency check. When the TAx4 array is completed, its area will be comparable to that of the Pierre Auger Observatory, and TAx4 being in the Northern Hemisphere whereas the Pierre Auger Observatory is in the Southern Hemisphere, will enable possible anisotropies in the arrival of UHECRs to be proved or disproved, and the testing of whether UHECR production is dominated by a few nearby sources or more numerous distant ones. Together, both observatories will probe the detailed properties of hadronic interactions at energies three orders of magnitude higher than what is achievable in laboratory particle accelerators. More thorough investigations from space will be possible with K-EUSO and POEMMA in the next 10–15 years.

Future all-sky monitors such as the LSST in the optical and the SKA in the radio, as well as the Fermi, Swift and the expected (in 2022) SVOM satellites at keV to GeV energies will provide rapid EM triggers and accurate sky localization together with the follow-up capability to study events such as black hole and neutron star mergers, supernovae, γ -ray bursts, AGN flares and so on, in which cosmic rays, neutrinos and GWs are also expected to be emitted in varying amounts. The strength and combination of these different messengers is model dependent, and multiple triggers for different messengers, as well as model development and extensive simulations, will be the key for understanding the physics of these energetic sources.

Because of the complementary advantages and limitations of the different messengers, the key to fully exploiting the power of the new facilities lies in the multi-messenger approach. Cosmic rays provide unique information about accelerated particles well beyond terrestrial laboratory capabilities, as well as information about the source magnetic fields and total energetics, but they do not reach us from beyond ~100 Mpc and offer at best poor angular resolution. Neutrinos reach us from the most distant places in the Universe, and

probe the inner, denser regions of the most energetic and cataclysmic events, and ultrahigh-energy neutrinos, being intimately linked to UHECRs, can provide unique clues as to how the latter reach their enormous energies. GW observations probe the most compact regions of high-energy sources; the GW wave strain amplitude on Earth is directly proportional to the source compactness, measured in terms of GM/c^2R (where G is the gravitational constant, M is the source mass, c is the speed of light and R is the distance from the source to Earth), and the GW luminosity goes as the fifth power of the compactness. GWs provide excellent information about the black hole or neutron star masses, angular momenta and distances, and they will eventually be detected from the farthest distances and earliest epochs

in the Universe, but they have modest angular resolution at best, and do not probe the bulk of the stellar or baryonic mass of their sources. EM waves provide excellent angular resolution, velocity and redshift determination capabilities, but the opacity of matter prevents them from probing the inner, denser regions of astronomical sources, whereas at higher γ -ray frequencies they cannot reach us directly from the much greater distances probed by neutrinos or GWs.

Thus, combining several messengers maximizes their individual strengths, providing a formidable toolkit for probing the most dramatic astrophysical events and testing our physical theories of the Universe.

Published online 3 October 2019

1. Aartsen, M. G. et al. First observation of PeV-energy neutrinos with IceCube. *Phys. Rev. Lett.* **111**, 021103 (2013).
2. IceCube Collaboration Evidence for high-energy extraterrestrial neutrinos at the IceCube detector. *Science* **342**, 1242856 (2013).
3. Auger collaboration Highlights from the Pierre Auger Observatory (ICRC17). Preprint at <https://arxiv.org/abs/1710.09478> (2017).
4. Abbott, B. P. et al. Observation of gravitational waves from a binary black hole merger. *Phys. Rev. Lett.* **116**, 061102 (2016).
5. Pierre Auger Collaboration The Pierre Auger Cosmic Ray Observatory. *Nucl. Instrum. Methods Phys. Res. A* **798**, 172–213 (2015).
6. Abbasi, R. et al. Observation of the GZK cutoff by the HiRes experiment. *Phys. Rev. Lett.* **100**, 101101 (2008).
7. Greisen, K. End to the cosmic-ray spectrum? *Phys. Rev. Lett.* **16**, 748–750 (1966).
8. Zatsepin, G. T. & Kuz'min, V. A. Upper limit of the spectrum of cosmic rays. *Sov. J. Exp. Theor. Phys. Lett.* **4**, 78 (1966).
9. Gerasimova, N. M. & Rozental, I. L. Influence of the nuclear photoeffect on the primary cosmic ray spectrum. *Sov. Phys. J. Exp. Theor. Phys.* **14**, 350 (1962).
10. Aab, A. et al. Evidence for a mixed mass composition at the 'ankle' in the cosmic-ray spectrum. *Phys. Lett. B* **762**, 288–295 (2016).
11. Gora, D. (for the Pierre Auger Collaboration) The Pierre Auger observatory: review of latest results and perspectives. Preprint at [ArXiv https://arxiv.org/abs/1811.00343](https://arxiv.org/abs/1811.00343) (2018).
12. Petrerá, S. Recent results from the Pierre Auger observatory. Preprint at [ArXiv https://arxiv.org/abs/1903.00529](https://arxiv.org/abs/1903.00529) (2019).
13. Kawai, H. et al. Telescope array experiment. *Nucl. Phys. B Proc. Suppl.* **175**, 221–226 (2008).
14. Telescope Array Collaboration et al. Mass composition of ultra-high-energy cosmic rays with the telescope array surface detector data. Preprint at [ArXiv https://arxiv.org/abs/1808.03680](https://arxiv.org/abs/1808.03680) (2018).
15. AbuZayyad, T. et al. The energy spectrum of cosmic rays at the highest energies. *JPS Conf. Proc.* **19**, 011003 (2018).
16. IceCube Collaboration. et al. First year performance of the IceCube neutrino telescope. *Astropart. Phys.* **26**, 155–173 (2006).
17. Kistler, M. D. & Laha, R. Multi-PeV signals from a new astrophysical neutrino flux beyond the glashow resonance. *Phys. Rev. Lett.* **120**, 241105 (2018).
18. Halzen, F. High-energy neutrino astrophysics. *Nat. Phys.* **13**, 232–238 (2017).
19. Ahlers, M. & Halzen, F. Opening a new window onto the universe with IceCube. *Prog. Part. Nucl. Phys.* **102**, 73–88 (2018).
20. IceCube Collaboration et al. The IceCube neutrino observatory — contributions to ICRC 2017 part I: searches for the sources of astrophysical neutrinos. Preprint at [ArXiv https://arxiv.org/abs/1710.01179](https://arxiv.org/abs/1710.01179) (2017).
21. Illuminati, G. Latest results from the ANTARES neutrino telescope and prospects for KM3Net-ARCA. *Nuovo Cimento C* **41**, 134 (2019).
22. Baikal-GVD Collaboration et al. Baikal-GVD: status and prospects. Preprint at [ArXiv https://arxiv.org/abs/1808.10353](https://arxiv.org/abs/1808.10353) (2018).
23. Allison, P. et al. Constraints on the diffuse high-energy neutrino flux from the third flight of ANITA. Preprint at [ArXiv https://arxiv.org/abs/1803.02719](https://arxiv.org/abs/1803.02719) (2018).
24. Aab, A. et al. Improved limit to the diffuse flux of ultrahigh energy neutrinos from the Pierre Auger Observatory. *Phys. Rev. D* **91**, 092008 (2015).
25. Abbott, B. P. et al. LIGO: the Laser Interferometer Gravitational-Wave Observatory. *Rep. Prog. Phys.* **72**, 076901 (2009).
26. Acernese, F. et al. Advanced Virgo: a second-generation interferometric gravitational wave detector. *Class. Quantum Gravity* **32**, 024001 (2015).
27. The LIGO Scientific Collaboration & the Virgo Collaboration. GWTC-1: a gravitational-wave transient catalog of compact binary mergers observed by LIGO and Virgo during the first and second observing runs. Preprint at [ArXiv https://arxiv.org/abs/1811.12907](https://arxiv.org/abs/1811.12907) (2018).
28. Connaughton, V. et al. Fermi GBM observations of LIGO gravitational wave event GW150914. Preprint at [ArXiv https://arxiv.org/abs/1602.03920](https://arxiv.org/abs/1602.03920) (2016).
29. Thompson, D. J. Space detectors for gamma rays (100 MeV–100 GeV): from EGRET to Fermi LAT. *C. R. Phys.* **16**, 600–609 (2015).
30. Montaruli, T. Gamma-rays and their future. Preprint at [ArXiv https://arxiv.org/abs/1902.10484](https://arxiv.org/abs/1902.10484) (2019).
31. Salesa Greus, F. Gamma-ray astronomy with the HAWC observatory. In *Proc. XXXVIII Polish Astronomical Society Meeting Vol. 7* (ed. Rozanska, A.) 316–321 (Polish Astronomical Society, 2018).
32. Casanova, S. Highlights from the HAWC telescope. In *Fourteenth Marcel Grossmann Meeting — MG14* (eds Bianchi, M., Jansen, R. T. & Ruffini, R.) 3303–3306 (World Scientific, 2018).
33. Davis, R. Nobel lecture: a half-century with solar neutrinos. *Rev. Mod. Phys.* **75**, 985–994 (2003).
34. Koshiha, M. Nobel lecture: birth of neutrino astrophysics. *Rev. Mod. Phys.* **75**, 1011–1020 (2003).
35. Hirata, K. et al. Observation of a neutrino burst from the supernova SN1987A. *Phys. Rev. Lett.* **58**, 1490–1493 (1987).
36. Alexeyev, E. N., Alexeyeva, L. N., Krivosheina, I. V. & Volchenko, V. I. Detection of the neutrino signal from SN 1987A in the LMC using the INR Baksan underground scintillation telescope. *Phys. Lett. B* **205**, 209–214 (1988).
37. Haines, T. et al. Neutrinos from SN1987a in the IMB detector. *Nucl. Instrum. Methods Phys. Res. A* **264**, 28–31 (1988).
38. Ackermann, M. et al. The spectrum of isotropic diffuse gamma-ray emission between 100 MeV and 820 GeV. *Astrophys. J.* **799**, 86 (2015).
39. Ackermann, M. Resolving the extragalactic γ -ray background above 50 GeV with the Fermi large area telescope. *Phys. Rev. Lett.* **116**, 151105 (2016).
40. Fang, K. & Murase, K. Linking high-energy cosmic particles by black-hole jets embedded in large-scale structures. *Nat. Phys.* **14**, 396–398 (2018).
41. Murase, K. & Waxman, E. Constraining high-energy cosmic neutrino sources: implications and prospects. *Phys. Rev. D* **94**, 103006 (2016).
42. Murase, K., Ahlers, M. & Lacki, B. C. Testing the hadronic origin of PeV neutrinos observed with IceCube. *Phys. Rev. D* **88**, 121301 (2013).
43. Murase, K., Guetta, D. & Ahlers, M. Hidden cosmic-ray accelerators as an origin of TeV–PeV cosmic neutrinos. *Phys. Rev. Lett.* **116**, 071101 (2016).
44. Ahlers, M. & Murase, K. Probing the galactic origin of the IceCube excess with gamma rays. *Phys. Rev. D* **90**, 023010 (2014).
45. Abbasi, R. et al. An absence of neutrinos associated with cosmic-ray acceleration in γ -ray bursts. *Nature* **484**, 351–354 (2012).
46. Aartsen, M. G. et al. Search for prompt neutrino emission from gamma-ray bursts with IceCube. *Astrophys. J. Lett.* **805**, L5 (2015).
47. Aartsen, M. G. et al. Constraints on minute-scale transient astrophysical neutrino sources. Preprint at [ArXiv https://arxiv.org/abs/1807.11402](https://arxiv.org/abs/1807.11402) (2018).
48. Mészáros, P. & Waxman, E. TeV neutrinos from successful and choked gamma-ray bursts. *Phys. Rev. Lett.* **87**, 171102–17110 (2001).
49. Murase, K. & Ioka, K. TeV–PeV neutrinos from low-power gamma-ray burst jets inside stars. *Phys. Rev. Lett.* **111**, 121102 (2013).
50. Abbott, B. et al. Search for gravitational waves associated with the gamma ray burst GRB030329 using the LIGO detectors. *Phys. Rev. D* **72**, 042002 (2005).
51. Abbott, B. et al. Astrophysically triggered searches for gravitational waves: status and prospects. *Class. Quantum Gravity* **25**, 114051 (2008).
52. Kanner, J. et al. LOOC UP: locating and observing optical counterparts to gravitational wave bursts. *Class. Quantum Gravity* **25**, 184034 (2008).
53. Abbott, B. et al. Implications for the origin of GRB 070201 from LIGO observations. *Astrophys. J.* **681**, 1419–1430 (2008).
54. Abbott, B. P. et al. Gravitational waves and gamma-rays from a binary neutron star merger: GW170817 and GRB 170817 A. *Astrophys. J. Lett.* **848**, L13 (2017).
55. The LIGO Scientific Collaboration et al. Properties of the binary neutron star merger GW170817. *Phys. Rev. X* **9**, 011001 (2019).
56. The LIGO Scientific Collaboration et al. GW170817: measurements of neutron star radii and equation of state. *Phys. Rev. Lett.* **121**, 161101 (2018).
57. Troja, E. et al. The X-ray counterpart to the gravitational wave event GW 170817. Preprint at [ArXiv https://arxiv.org/abs/1710.05433](https://arxiv.org/abs/1710.05433) (2017).
58. Coulter, D. A. et al. Swope supernova survey 2017a (SSS17a), the optical counterpart to a gravitational wave source. *Science* **358**, 1556–1558 (2017).
59. Kasliwal, M. M. et al. Illuminating gravitational waves: a concordant picture of photons from a neutron star merger. *Science* **358**, 1559–1565 (2017).
60. Abbott, B. P. et al. Multi-messenger observations of a binary neutron star merger. *Astrophys. J.* **848**, L12 (2017).
61. Margutti, R. et al. The electromagnetic counterpart of the binary neutron star merger LIGO/Virgo GW170817. V. Rising X-ray emission from an off-axis jet. *Astrophys. J.* **848**, L20 (2017).
62. Weiss, R. LIGO and the discovery of gravitational waves. I. Nobel lecture, December 8, 2017. *Ann. Phys.* **531**, 1800349 (2019).
63. Barish, B. C. LIGO and gravitational waves II: Nobel lecture, December 8, 2017. *Ann. Phys.* **531**, 1800357 (2019).
64. Thorne, K. S. LIGO and gravitational waves, III: Nobel lecture, December 8, 2017. *Ann. Phys.* **531**, 1800350 (2019).
65. IceCube Collaboration et al. Multimessenger observations of a flaring blazar coincident with

- high-energy neutrino IceCube-170922A. *Science* **361**, eaat1378 (2018).
66. Mirzoyan, R. First-time detection of VHE gamma rays by MAGIC from a direction consistent with the recent EHE neutrino event IceCube-170922A. *Astron. Telegr.* 10817 (2017).
67. Keivani, A. et al. A multimessenger picture of the flaring blazar TXS 0506+056: implications for high-energy neutrino emission and cosmic ray acceleration. *Astrophys. J.* **864**, 84 (2018).
68. Fox, D. B. et al. Joint swift XRT and NuSTAR observations of TXS 0506+056. *Astron. Telegr.* 10845 (2017).
69. Padovani, P., Oikonomou, F., Petropoulou, M., Giommi, P. & Resconi, E. TXS 0506+056, the first cosmic neutrino source, is not a BL Lac. *Mon. Not. R. Astron. Soc.* **484**, L104–L108 (2019).
70. IceCube Collaboration Neutrino emission from the direction of the blazar TXS 0506+056 prior to the IceCube-170922A alert. *Science* **361**, 147–151 (2018).
71. Gao, S., Fedynitch, A., Winter, W. & Pohl, M. Modelling the coincident observation of a high-energy neutrino and a bright blazar flare. *Nat. Astron.* **3**, 88–92 (2019).
72. Cerruti, M. et al. Leptohadronic single-zone models for the electromagnetic and neutrino emission of TXS 0506+056. *Mon. Not. R. Astron. Soc.* **483**, L12–L16 (2019).
73. Aartsen, M. G. et al. The contribution of Fermi-2LAC blazars to diffuse TeV–PeV neutrino flux. *Astrophys. J.* **835**, 45 (2017).
74. Perna, R., Lazzati, D. & Giacomazzo, B. Short gamma-ray bursts from the merger of two black holes. *Astrophys. J. Lett.* **821**, L18 (2016).
75. Murase, K., Kashiyama, K., Mészáros, P., Shoemaker, I. & Senno, N. Ultrafast outflows from black hole mergers with a minidisk. *Astrophys. J. Lett.* **822**, L9 (2016).
76. Bartos, I. et al. Gravitational-wave localization alone can probe origin of stellar-mass black hole mergers. *Nat. Commun.* **8**, 831 (2017).
77. Ford, K. E. S. et al. AGN (and other) astrophysics with gravitational wave events. Preprint at <https://arxiv.org/abs/1903.09529> (2019).
78. Albert, A. et al. Search for multimessenger sources of gravitational waves and high-energy neutrinos with advanced LIGO during its first observing run, ANTARES, and IceCube. *Astrophys. J.* **870**, 134 (2019).
79. Bird, S. et al. Did LIGO detect dark matter? *Phys. Rev. Lett.* **116**, 201301 (2016).
80. Magee, R. & Hanna, C. Disentangling the potential dark matter origin of LIGO's black holes. Preprint at <https://arxiv.org/abs/1706.04947> (2017).
81. Carr, B. Primordial black holes as dark matter and generators of cosmic structure. Preprint at <https://arxiv.org/abs/1901.07803> (2019).
82. Bartos, I., Finley, C., Corsi, A. & Márka, S. Observational constraints on multimessenger sources of gravitational waves and high-energy neutrinos. *Phys. Rev. Lett.* **107**, 251101 (2011).
83. Ando, S. et al. Colloquium: multimessenger astronomy with gravitational waves and high-energy neutrinos. *Rev. Mod. Phys.* **85**, 1401–1420 (2013).
84. Kimura, S. S., Murase, K., Mészáros, P. & Kiuchi, K. High-energy neutrino emission from short gamma-ray bursts: prospects for coincident detection with gravitational waves. *Astrophys. J. Lett.* **848**, L4 (2017).
85. Kimura, S. S. et al. Transejecta high-energy neutrino emission from binary neutron star mergers. *Phys. Rev. D* **98**, 043020 (2018).
86. Hooper, D., Linden, T. & Vieregg, A. Active galactic nuclei and the origin of IceCube's diffuse neutrino flux. Preprint at <https://arxiv.org/abs/1810.02823> (2018).
87. Murase, K., Oikonomou, F. & Petropoulou, M. Blazar flares as an origin of high-energy cosmic neutrinos? *Astrophys. J.* **865**, 124 (2018).
88. The LIGO Scientific Collaboration & The Virgo Collaboration Binary black hole population properties inferred from the first and second observing runs of advanced LIGO and Advanced Virgo. Preprint at <https://arxiv.org/abs/1811.12940> (2018).
89. IceCube Collaboration, Pierre Auger Collaboration & Telescope Array Collaboration. Search for correlations between the arrival directions of IceCube neutrino events and ultrahigh-energy cosmic rays detected by the Pierre Auger observatory and the telescope array. *Jour. Cosmol. Astro-Part. Phys.* **1**, 037 (2016).
90. Moharana, R. & Razaque, S. Angular correlation of cosmic neutrinos with ultrahigh-energy cosmic rays and implications for their sources. *J. Cosmol. Astropart. Phys.* **8**, 014 (2015).
91. Aloisio, R., Berezhinsky, V. & Blasi, P. Ultra high energy cosmic rays: implications of Auger data for source spectra and chemical composition. *J. Cosmol. Astropart. Phys.* **2014**, 020 (2014).
92. Alves Batista, R., de Almeida, R. M., Lago, B. & Kotera, K. Cosmogenic photon and neutrino fluxes in the Auger era. *J. Cosmol. Astropart. Phys.* **1**, 002 (2019).
93. Murase, K. & Fukugita, M. Energetics of high-energy cosmic radiations. *Phys. Rev. D* **99**, 063012 (2019).
94. Radice, D. et al. Binary neutron star mergers: mass ejection, electromagnetic counterparts, and nucleosynthesis. *Astrophys. J.* **869**, 130 (2018).
95. Glas, R., Just, O., Janka, H. T. & Obergaulinger, M. Three-dimensional core-collapse supernova simulations with multidimensional neutrino transport compared to the ray-by-ray-plus approximation. *Astrophys. J.* **873**, 45 (2019).
96. Radice, D., Morozova, V., Burrows, A., Vartanyan, D. & Nagakura, H. Characterizing the gravitational wave signal from core-collapse supernovae. *Astrophys. J.* **876**, L9 (2019).
97. Seckel, D. & Stanev, T. Neutrinos: the key to UHE cosmic rays. *Phys. Rev. Lett.* **95**, 141101 (2005).
98. Kotera, K. & Olinto, A. V. The astrophysics of ultrahigh-energy cosmic rays. *Annu. Rev. Astron. Astrophys.* **49**, 119–153 (2011).
99. Globus, N., Allard, D., Parizot, E. & Piran, T. Probing the extragalactic cosmic-ray origin with gamma-ray and neutrino backgrounds. *Astrophys. J.* **839**, L22 (2017).
100. Gorham, P. W. et al. Observation of an unusual upward-going cosmic-ray-like event in the third flight of ANITA. Preprint at <https://arxiv.org/abs/1803.05088> (2018).
101. Alvarez-Muñiz, J. et al. Comprehensive approach to tau-lepton production by high-energy tau neutrinos propagating through the Earth. *Phys. Rev. D* **97**, 023021 (2018).
102. Romero-Wolf, A. et al. Upward-pointing cosmic-ray-like events observed with ANITA. Preprint at <https://arxiv.org/abs/1810.00439> (2018).
103. Connolly, A., Allison, P. & Banerjee, O. On ANITA's sensitivity to long-lived, charged massive particles. Preprint at <https://arxiv.org/abs/1807.08892> (2018).
104. Fox, D. B. et al. The ANITA anomalous events as signatures of a beyond standard model particle, and supporting observations from IceCube. Preprint at <https://arxiv.org/abs/1809.09615> (2018).
105. Dagoneau, N., Cordier, B., Schanne, S. & Gros, A. Detection capability of ultra-long gamma-ray bursts with the ECLAIRs telescope aboard the SVOM mission under development. In *42nd COSPAR Scientific Assembly Vol. 42 E1.17–46–18* (2018).
106. Zhang, D. et al. Energy response of GECAM gamma-ray detector based on LaBr₃:Ce and SiPM array. *Nucl. Instrum. Methods Phys. Res. A* **921**, 8–13 (2019).
107. Yuan, W. et al. Einstein Probe — a small mission to monitor and explore the dynamic X-ray universe. Preprint at <https://arxiv.org/abs/1506.07735> (2015).
108. Sagiv, I. et al. Science with a wide-field UV transient explorer. *Astron. J.* **147**, 79 (2014).
109. Yacobi, L. et al. The gamma-ray transient monitor for ISS-TAO: new directional capabilities. *Proc. SPIE* **10699**, 106995U (2018).
110. Patterson, M. T. et al. The Zwicky Transient Facility alert distribution system. *Publ. Astron. Soc. Pac.* **131**, 018001 (2019).
111. Kochanek, C. S. et al. The All-Sky Automated Survey for Supernovae (ASAS-SN) light curve server v1.0. *Publ. Astron. Soc. Pac.* **129**, 104502 (2017).
112. Cherenkov Telescope Array Consortium et al. Science with the Cherenkov Telescope Array. Preprint at <https://arxiv.org/abs/1709.07997> (2017).
113. Di Sciascio, G. & LHAASO Collaboration The LHAASO experiment: from gamma-ray astronomy to cosmic rays. *Nucl. Part. Phys. Proc.* **279**, 166–173 (2016).
114. LSST Science Collaboration et al. Science-driven optimization of the LSST observing strategy. Preprint at <https://arxiv.org/abs/1708.04058> (2017).
115. McPherson, A. M. et al. Square Kilometer Array project status report. *Proc. SPIE* **10700**, 107000Y (2018).
116. Sanders, G. H. The Thirty Meter Telescope (TMT): an international observatory. *J. Astrophys. Astron.* **34**, 81–86 (2013).
117. Varela, A. M. et al. European extremely large telescope site characterization III: ground meteorology. *Publ. Astron. Soc. Pac.* **126**, 412–431 (2014).
118. Johns, M. et al. Giant Magellan Telescope: overview. *Proc. SPIE* **8444**, 84441H (2012).
119. Nandra, K. in *The X-ray Universe 2011* (eds Ness, J.-U. & Ehle, M.) 022 (2011).
120. Amati, L. et al. The THESEUS space mission concept: science case, design and expected performances. *Adv. Space Res.* **62**, 191–244 (2018).
121. Moiseev, A. & AMEGO Team All-Sky Medium Energy Gamma-ray Observatory (AMEGO). *Int. Cosm. Ray Conf.* **35**, 798–803 (2017).
122. Predehl, P. et al. eROSITA on SRG. *Proc. SPIE* **9905**, 99051K (2016).
123. IceCube-Gen2 Collaboration et al. The IceCube neutrino observatory — contributions to ICRC 2017 part VI: IceCube-Gen2, the next generation neutrino observatory. Preprint at <https://arxiv.org/abs/1710.01207> (2017).
124. The KM3NeT Collaboration et al. Sensitivity of the KM3NeT/ARCA neutrino telescope to point-like neutrino sources. Preprint at <https://arxiv.org/abs/1810.08499> (2018).
125. Baikal-GVD Collaboration et al. Baikal-GVD: status and prospects. Preprint at <https://arxiv.org/abs/1808.10353> (2018).
126. Hyper-Kamiokande Proto-Collaboration et al. Hyper-kamiokande design report. Preprint at <https://arxiv.org/abs/1805.04163> (2018).
127. Migenda, J. & Hyper-Kamiokande Proto-Collaboration Astroparticle physics in hyper-kamiokande. In *Proc. European Physical Society Conference on High Energy Physics. 5–12 July, 20* (2017).
128. Barwick, S. W. et al. Radio detection of air showers with the ARIANNA experiment on the Ross Ice Shelf. *Astropart. Phys.* **90**, 50–68 (2017).
129. Allison, P. et al. Performance of two askaryan radio array stations and first results in the search for ultrahigh energy neutrinos. *Phys. Rev. D* **93**, 082003 (2016).
130. GRAND Collaboration et al. The Giant Radio Array for Neutrino Detection (GRAND): science and design. Preprint at <https://arxiv.org/abs/1810.09994> (2018).
131. Olinto, A. V. et al. POEMMA: probe of extreme multimessenger astrophysics. *Int. Cosm. Ray Conf.* **301**, 542 (2017).
132. Nepomuk Otte, A. Trinity: an air-shower imaging system for the detection of cosmogenic neutrinos. Preprint at <https://arxiv.org/abs/1811.09287> (2018).
133. Veberic, D. (ed.) *The Pierre Auger Observatory: Contributions to the 35th International Cosmic Ray Conference (ICRC 2017)* (2017).
134. Sagawa, H. & Telescope Array Collaboration Telescope array extension: TAx4. In *34th International Cosmic Ray Conference (ICRC2015) Vol. 34* 657 (2015).
135. Casolino, M. et al. KLYPVE-EUSO: science and UHECR observational capabilities. *Proc. Sci. ICRC2017*, 368 (2018).
136. Winchen, T. et al. Cosmic ray physics with the LOFAR radio telescope. Preprint at <https://arxiv.org/abs/1903.08474> (2019).
137. Seo, E. S. et al. Cosmic ray energetics and mass for the international space station (ISS-CREAM). *Adv. Space Res.* **53**, 1451–1455 (2014).
138. Zhang, S. N. et al. The high energy cosmic-radiation detection (HERD) facility onboard China's space station. *Proc. SPIE* **9144**, 91440X (2014).
139. Fujii, T. et al. The FAST project — a next generation UHECR observatory. In *European Physical Journal Web of Conferences Vol. 136* 02015 (2017).
140. Gaisser, T. K., Stanev, T. & Tilav, S. Cosmic ray energy spectrum from measurements of air showers. *Front. Phys.* **8**, 748–758 (2013).
141. Abbott, B. P. et al. Prospects for observing and localizing gravitational-wave transients with Advanced LIGO, Advanced Virgo and KAGRA. *Living Rev. Relativ.* **21**, 3 (2018).
142. Abbott, B. P. et al. Exploring the sensitivity of next generation gravitational wave detectors. *Class. Quantum Gravity* **34**, 044001 (2017).
143. Sathyaprakash, B. et al. Scientific objectives of einstein telescope. *Class. Quantum Gravity* **29**, 124013 (2012).
144. Abbott, B. P. et al. Exploring the sensitivity of next generation gravitational wave detectors. *Class. Quantum Gravity* **34**, 044001 (2017).
145. Klein, A. et al. Science with the space-based interferometer eLISA: supermassive black hole binaries. *Phys. Rev. D* **93**, 024003 (2016).
146. Schutz, K. & Ma, C.-P. Constraints on individual supermassive black hole binaries from pulsar timing array limits on continuous gravitational waves. *Mon. Not. R. Astron. Soc.* **459**, 1737–1744 (2016).

147. Hobbs, G. & Dai, S. A review of pulsar timing array gravitational wave research. Preprint at *ArXiv* <https://arxiv.org/abs/1707.01615> (2017).
148. Arzoumanian, Z. et al. The NANOGrav 11 year data set: pulsar-timing constraints on the stochastic gravitational-wave background. *Astrophys. J.* **859**, 47 (2018).
149. Keivani, A., Ayala, H. & DeLaunay, J. Astrophysical multimessenger observatory network (AMON): science, infrastructure, and status. Preprint at *ArXiv* <https://arxiv.org/abs/1708.04724> (2017).
150. Ayala Solares, H. A. et al. The astrophysical multimessenger observatory network (AMON). Preprint at *ArXiv* <https://arxiv.org/abs/1903.08714> (2019).
151. Turley, C. F. et al. A coincidence search for cosmic neutrino and gamma-ray emitting sources using IceCube and Fermi-LAT public data. *Astrophys. J.* **863**, 64 (2018).
152. Countryman, S. et al. Low-latency algorithm for multi-messenger astrophysics (LLAMA) with gravitational-wave and high-energy neutrino candidates. Preprint at *ArXiv* <https://arxiv.org/abs/1901.05486> (2019).
153. Schutz, B. F. Gravitational-wave astronomy: delivering on the promises. *Phil. Trans. R. Soc. Lond. Ser. A* **376**, 20170279 (2018).
154. Mészáros, P. Astrophysical sources of high-energy neutrinos in the IceCube era. *Annu. Rev. Nucl. Part. Sci.* **67**, 45–67 (2017).
155. Shibata, M., Kiuchi, K. & Sekiguchi, Y.-i General relativistic viscous hydrodynamics of differentially rotating neutron stars. *Phys. Rev. D* **95**, 083005 (2017).
156. Easter, P. J., Lasky, P. D., Casey, A. R., Rezzolla, L. & Takami, K. Computing fast and reliable gravitational waveforms of binary neutron star merger remnants. Preprint at *ArXiv* <https://arxiv.org/abs/1811.11183> (2018).
157. Parsotan, T., López-Cámara, D. & Lazzati, D. Photospheric emission from variable engine gamma-ray burst simulations. *Astrophys. J.* **869**, 103 (2018).
158. van Eerten, H. Gamma-ray burst afterglow blast waves. *Int. J. Mod. Phys. D* **27**, 1842002–1842314 (2018).
159. Senno, N., Murase, K. & Mészáros, P. Choked jets and low-luminosity gamma-ray bursts as hidden neutrino sources. *Phys. Rev. D* **93**, 083003 (2016).
160. Hotokezaka, K., Beniamini, P. & Piran, T. Neutron star mergers as sites of r-process nucleosynthesis and short gamma-ray bursts. *Int. J. Mod. Phys. D* **27**, 1842005 (2018).
161. Biehl, D., Boncioli, D., Fedynitch, A. & Winter, W. Cosmic ray and neutrino emission from gamma-ray bursts with a nuclear cascade. *Astron. Astrophys.* **611**, A101 (2018).
162. Lu, J.-S., Li, Y.-F. & Zhou, S. Getting the most from the detection of galactic supernova neutrinos in future large liquid-scintillator detectors. *Phys. Rev. D* **94**, 023006 (2016).
163. Beacom, J. F. The diffuse supernova neutrino background. *Annu. Rev. Nucl. Part. Sci.* **60**, 439–462 (2010).
164. Tamborra, I. & Murase, K. Neutrinos from supernovae. *Space Sci. Rev.* **214**, 31 (2018).
165. Wild, W. Cherenkov telescope array (CTA): building the world's largest ground-based gamma-ray observatory. *Proc. SPIE* **10700**, 107000X (2018).
166. Design concepts for the Cherenkov Telescope Array CTA: an advanced facility for ground-based high-energy gamma-ray astronomy. *Experimental Astronomy* **32**, 193–316 (2011).
167. Spiering, C. High energy neutrino astronomy: where do we stand, where do we go? *Physics of Particles and Nuclei* **49**, 497–507 (2018).
168. Kimura, S. S., Murase, K. & Mészáros, P. Super-knee cosmic rays from galactic neutron star merger remnants. *Astrophys. J.* **866**, 51 (2018).
169. Guépin, C., Kotera, K., Barausse, E., Fang, K. & Murase, K. Ultra-high energy cosmic rays and neutrinos from tidal disruptions by massive black holes. Preprint at *ArXiv* <https://arxiv.org/abs/1711.11274> (2017).
170. Biehl, D., Boncioli, D., Lunardini, C. & Winter, W. Tidally disrupted stars as a possible origin of both cosmic rays and neutrinos at the highest energies. <https://arxiv.org/abs/1711.03555> (2017).
171. Senno, N., Murase, K. & Meszaros, P. High-energy neutrino flares from X-ray bright and dark tidal disruptions events. <https://arxiv.org/abs/1612.00918> (2016).
172. Wang, X.-Y. & Liu, R.-Y. Tidal disruption jets of supermassive black holes as hidden sources of cosmic rays: explaining the IceCube TeV-PeV neutrinos. <https://arxiv.org/abs/1512.08596> (2015).
173. Klein, A. et al. Science with the space-based interferometer eLISA: supermassive black hole binaries. *Phys. Rev. D* **93**, 024003 (2016).
174. Murase, K. & Bartos, I. High-energy multi-messenger transient astrophysics. Preprint in *ArXiv* <https://arxiv.org/abs/1907.12506> (2019).

Acknowledgements

The authors thank S. Coutu, D. Cowen, M. Mostafá and B. Sathyaprakash for useful discussions and comments.

Author contributions

The authors contributed equally to all aspects of the article.

Competing interests

The authors declare no competing interests.

Publisher's note

Springer Nature remains neutral with regard to jurisdictional claims in published maps and institutional affiliations.